Study of O-phosphorylation sites in proteins involved in photosynthesis-related processes in *Synechocystis* sp. strain PCC 6803: application of the SRM approach

*Angeleri Martina, Muth-Pawlak Dorota, Aro Eva-Mari, Battchikova Natalia**

**Corresponding author. Tel: +358-2-3338078, e-mail: natbat@utu.fi*

Molecular Plant Biology, Department of Biochemistry, University of Turku, FI-20014 Turku, Finland

ABSTRACT

O-phosphorylation has been shown in photosynthesis-related proteins in a cyanobacterium *Synechocystis* sp. strain PCC 6803 (thereafter *Synechocystis* 6803) suggesting that phosphorylation of S,T and Y residues might be important in photosynthesis-related processes. Investigation of biological roles of these phosphorylation events requires confident knowledge of the phosphorylated sites and prospects for their individual assessment. We performed phosphoproteomic analysis of *Synechocystis* 6803 using TiO_2 enrichment of the phosphopeptides followed by LC-MS/MS and discovered 367 phosphorylation sites in 190 proteins participating in various cellular functions. Further, we focused on the large group of phosphoproteins which are involved in light harvesting, photosynthesis-driven electron flow, photoprotection and CO_2 fixation. The SRM approach was applied to verify/improve assignments of phosphorylation sites in these proteins and to investigate possibilities for analysis of phosphopeptide isomers. The SRM assays were designed for peptides comprising 45 phosphorylation sites. The assays contain peptide iRT values and Q1/Q3 transitions comprising those discriminating between phosphopeptide isoforms. The majority of investigated phosphopeptides and phosphorylated isoforms could be individually assessed with the SRM technique. The assays could be potentially used in future quantitative

studies to evaluate an extent of phosphorylation in photosynthesis-related proteins in *Synechocystis* 6803 cells challenged with various environmental stresses.

Keywords: Cyanobacteria, *Synechocystis* 6803, photosynthesis, protein phosphorylation, phosphoproteomics, phosphoproteins, phosphopeptides, phosphopeptide isoforms, SRM, selected reaction monitoring.

INTRODUCTION

Cyanobacteria, or blue-green algae, are prokaryotic microorganisms that perform oxygenic photosynthesis, the process that transforms energy of sunlight into chemical energy (ATP and NADPH) with a concomitant production of oxygen. Photosynthesis drives carbon fixation, a conversion of inorganic carbon in the form of atmospheric CO_2 into organic compounds utilized in various cellular metabolic reactions. These two fundamental processes are already exploited in "green" industrial applications directed to production of biofuels and various high-value biological compounds in cyanobacteria[1] and further developments in this field will stimulate generation of clean energy and important chemicals from renewable resources helping to build a sustainable bioeconomy. An intelligent design of cyanobacteria with the synthetic biology approach for industrial purposes requires the profound knowledge how cells control energy distribution between the photosynthetic machinery and alternative electron flow pathways as well as how they regulate and optimize downstream processes of carbon metabolism.

The large protein complexes that govern photosynthesis and carbon fixation in cyanobacteria are phycobilisomes (PBS), Photosystem I (PSI), Photosystem II (PSII) and Cytochrome b_6f (Cyt b_6f) complexes together with ATPase and Ribulose-1,5-bisphosphate carboxylase/oxygenase (Rubisco). Their structures and functions have been well characterized in cyanobacteria *via* a broad assortment of scientific approaches as biochemistry, biophysics, reverse

genetics, proteomics, X-ray studies, high resolution imaging, *etc*; schematically, they are shown in Figure 1. PBS are bulky hemidiscoidal multisubunit pigment-proteins complexes that serve as the major light-harvesting antenna in cyanobacteria.[2] PSII, Cyt b_6f and PSI are the basis of the photosynthetic electron transfer machinery; together with ATP synthase, they function as large multi-protein complexes integrated into the thylakoid membrane.[3,4] Rubisco, the primary acceptor of CO_2, is encapsulated into carboxysomes, distinct cyanobacterial compartments where the carbon fixation occurs.[5] Many other proteins maintain and support these processes by connecting the electron flow between the big complexes and participating in photoprotection and repair of fragile photosynthetic complexes, balancing linear and alternative electron flows and tuning the production of NADPH and ATP to the strength of available electron sinks.

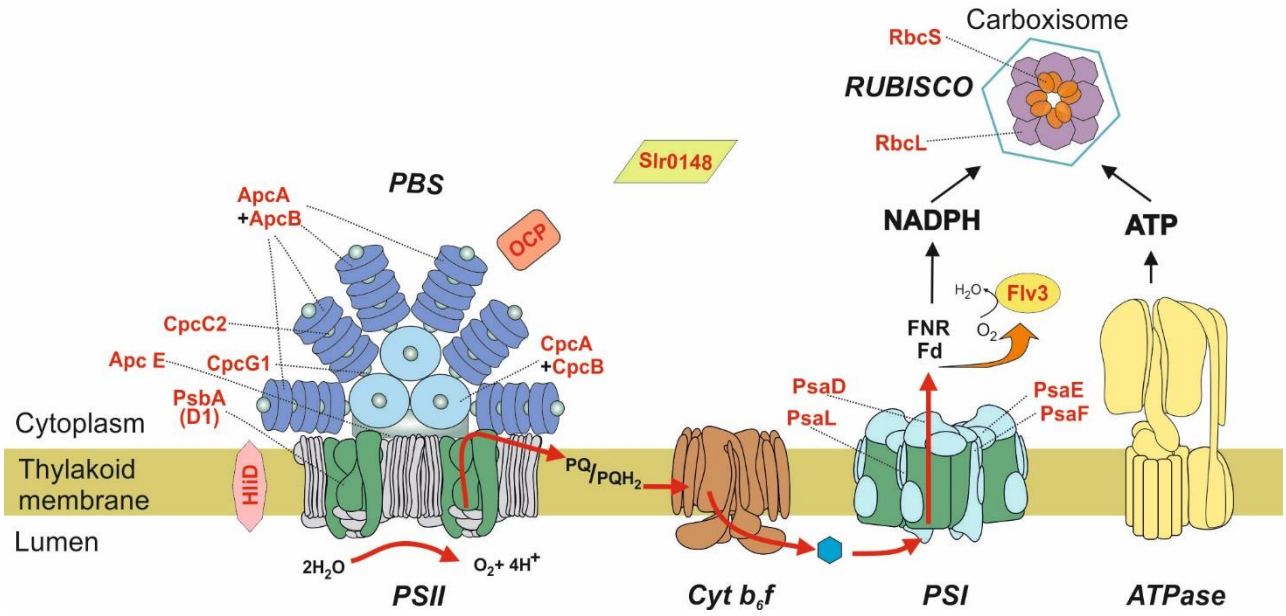

Figure 1: Schematic representation of the photosynthetic apparatus in cyanobacteria. Photosynthesis-driven electron flow is shown by red arrows. PQ: plastoquinone. Multiprotein complexes involved in light harvesting, photosynthesis and CO_2 fixation are indicated by bold italic. Their subunits and other photosynthesis-related proteins that contain phosphopeptides studied in the present paper are shown in red.

It has been established that light harvesting, photosynthesis-driven electron flow and following conversion of CO_2 are strictly controlled in the cells and optimized to existing environmental conditions. The dynamics of mechanisms regulating these processes was extensively studied with quantitative label-based and label-free proteomic techniques which revealed wide-ranging up- and down-regulation of various proteins in a response to changes in environmental conditions.[6-9] Beside alterations in gene expression, accumulation and activity of proteins can be finely controlled and modulated at the post-transcriptional level. Reversible protein phosphorylation is one of the most widespread post-translation modification (PTM) which is involved in regulation of diverse cellular processes including adjustment of various metabolic reactions, signal transduction, transcription, translation, homeostasis, *etc*.[10] Protein phosphorylation may occur at several amino acid residues. Some time ago, regulation based on modification at S/T/Y residues, or O-phosphorylation, has been considered as an eukaryotic feature whereas the use of two-component systems exploiting phosphorylation of H and D in histidine kinases and response regulators was thought to be a principal way for signal transduction in bacteria.[11] However, phosphoproteomic analyses on several bacteria including *E. coli,*[12] *Bacillus subtilis,*[13,14] *Pseudomonas sp.,*[15] *Streptomyces coelicolor*[16] and others demonstrated that the eukaryotic-type protein phosphorylation takes place also in prokaryotes.

Protein phosphorylation in cyanobacteria was first revealed by J.F.Allen and coworkers by [^{32}P] ATP labeling of *Synechococcus* 6301 *in vivo* and *in vitro*.[17,18] Moreover, the authors showed that phosphorylation occurred in a light-dependent fashion indicating that this PTM is directly or indirectly linked to the cyanobacterial photosynthetic machinery. Further studies performed using pS- and pT-specific antibodies showed O-phosphorylation of β-phycocyanin,[19] PBS linker proteins and ferredoxin:$NADP^+$ oxidoreductase (FNR);[20] however, a modification site often remained unknown. The occurrence of O-phosphorylation in proteins which participate in the capture of light

and photosynthetic linear electron transfer indicates that this PTM might be also important in regulation/optimization of photosynthesis, along with some histidine kinases with phytochrome-like features that have been suggested as potential sensors of light.[21]

Cyanobacteria are progenitors of chloroplasts, specific organelles that perform photosynthesis in eukaryotic photosynthetic organisms, for example, algae and green plants. Many components in light-harvesting antennas and both photosystems in green plants were found to be targets of O-phosphorylation.[22-24] It is well established at present that O-phosphorylation is one of the major mechanisms that sense and react to changes in the energetic balance of chloroplasts.[25] In response to environmental cues, differential phosphorylation of chloroplast thylakoid membrane proteins regulates lateral migration, mobility and packing density, composition, stability and repair of the membrane protein complexes, as well as the whole macroscopic structure of thylakoids.[26] In contrast, significance and biological role of O-phosphorylation in cyanobacterial proteins involved in photosynthesis and carbon fixation remain an open question.

With the development of mass spectrometry techniques and their application in phosphoproteomic studies of complex samples, the large-scale exploration of S/T/Y phosphorylated proteins in cyanobacteria has become possible.[27--31] The analyses of cyanobacterial phosphoproteomes isolated from cells growing in various environmental conditions will trigger further studies to clarify biological roles of specific phosphorylation events and their importance for regulation of metabolic and signaling pathways including those related to photosynthesis.

A reliability in the identification of a phosphorylation site is principally important for these studies. Although the disclosure of thousands of phosphopeptides by liquid chromatography – tandem mass spectrometry (LC-MS/MS) in complex samples is straightforward and relatively easy to perform, the assignment of phosphorylation often remains a challenge since phosphopeptides frequently occur in cells in non-stoichiometric amounts. The task to accurately localize a modification site becomes even more difficult when multiple potential phosphorylation sites are

present in the peptide sequence. Besides, when LC-MS/MS analyses are performed on complex samples, false identification do happen due to, for example, spectra inconsistencies, competing peptide fragmentation pathways and limitations in data interpretation software.[32] Despite many approaches were used in order to improve algorithms of the phosphorylation site assignment,[33-37] the problem remains and, currently, the manual validation of phosphopeptide spectra is recommended.[38-40]

In the present paper, we focus on photosynthesis-related phosphoproteins of the unicellular cyanobacterium *Synechocystis* sp. strain PCC 6803 (thereafter *Synechocystis* 6803). For their detection, we performed the in-depth phosphoproteomic analysis of *Synechocystis* 6803 using TiO_2 enrichment of phosphopeptides and LC-MS/MS analysis. Further, we investigated phosphopeptides detected in these proteins with the Selected Reaction Monitoring (SRM) approach[41-43] in order to improve/confirm identifications of phosphorylation sites[44- 46] and to create a reliable method for their accurate quantification in future studies. The designed SRM assays of phosphopeptides verified with specific transitions and characteristic iRT values are now available in the Panorama Public, https://panoramaweb.org

EXPERIMENTAL PROCEDURES

Cell growth conditions

Synechocystis sp. PCC 6803 glucose-tolerant strain[47] was grown in BG-11 medium[48] at 30°C under constant illumination of 50 µmol photons^{-2} s^{-1} in flasks constantly shaking at 110 rpm. To create high-carbon conditions (HC), BG-11 medium was supplemented with 10 mM of TES-KOH, pH 8.0, and cells were incubated in 3% CO_2. For low-carbon conditions (LC), buffering was performed with 10 mM of HEPES-NaOH, pH 7.5, carbonate was omitted from the medium, and cells were incubated in atmospheric air (0.04% CO_2). Cells were collected in the logarithmic phase, at

OD_{750}≈1, by centrifugation at 8000 rpm (7000 g) for 5 minutes at 4°C and washed by re-suspension in cold deionized water followed by centrifugation in the same conditions.

Protein isolation and digestion to peptides

Cell pellet was resuspended in a lysis buffer containing 8 M urea, 20 mM Tris-HCl pH 8.0, 100 mM NaCl, 1 mM EDTA, 1 mM EGTA, phosphatase inhibitors 10 mM NaF, 10 mM $Na_4P_2O_7$, 50 mM β-glycerophosphate, 5 mM of Na_3VO_4, and the protease inhibitor cocktail (Thermo Pierce™ Mini Tablets), 1 tablet per 10 ml of the solution. The density of the cell suspension corresponded to 1 g of a wet cell pellet in 15 ml of the lysis buffer. Resuspended cells were immediately lysed with a French press (Constant System LTD, Daventry, UK) applying 5 shots with a pressure of 40 kPsi. The crude extract was supplemented with 4% n-dodecyl β-D-maltoside, DM (Sigma) and 5 mM Tris(2-carboxyethyl)phosphine hydrochloride, TCEP (Sigma); the reduction of disulfide bonds was performed at room temperature (RT) for 20 min. Further, proteins were alkylated with 50 mM iodoacetamide, IAA (Sigma) in the dark at RT for 1 h. Cell debris was removed by centrifugation at 12000 rpm (15600g) for 25 min at RT. Proteins were purified as described in Wessel and Flügge,[49] with small modifications. Four volumes of methanol (MeOH), two volumes of chloroform, and three volumes of water were consequently added to cleared lysates, with 1-min vortex mixing after addition of every component. After centrifugation at 12000 rpm (15600g) for 10 min at RT, the upper yellowish phase was discarded. Three volumes of MeOH were added to the green bottom phase and greyish interphase, and proteins were precipitated by centrifugation in the same conditions. Proteins were dissolved in the buffer containing 8 M urea, 40 mM Tris-HCl pH 7.5, 5 mM NaF, 5 mM $Na_4P_2O_7$, 5 mM β-glycerophosphate, 5 mM of Na_3VO_4 and the protein concentration was determined with a Bradford assay (Bradford 1976). For a single analysis, 7-10 mg of a total *Synechocystis* protein was digested with TCPK-trypsin (Thermo Scientific, cat.no. 20233). Before trypsin digestion, proteins were diluted 5 times to decrease concentration of urea to

1.5 M, and $CaCl_2$ was added to final concentration of 1 mM to limit trypsin self-digestion. Reaction was performed at 30°C overnight.

Peptide fractionation for LC-MS/MS analysis

Following trypsin digestion, peptides were fractionated using three successive reverse phase chromatography steps using cartridges with reverse chromatography resins. First, peptide mixtures were loaded onto a tC2 cartridge (Waters, Sep-Pak Vac 3 cc, 500 mg) equilibrated with the 10mM ammonium bicarbonate (ABC) buffer; flow through with unbound peptides was collected. After washing the tC2 resin twice with the buffer, C2-bound peptides were eluted in three fractions, with 10%, 20% and 80% of acetonitrile (AcN) in 10 mM ABC. Second, flow through tC2 was loaded onto a C8 cartridge (Agilent, Sampli Q, Octyl, 500 mg) equilibrated with 10 mM ABC, and flow through was again collected. After washing, C8-bound peptides were eluted in two steps, with 15% and 80% AcN in 10 mM ABC. Third, flow through C8 was acidified with formic acid (FA) to pH 2-3 and loaded onto a C18 cartridge (Waters, Sep-Pak Vac 1 cc, 100 mg) equilibrated with 5% formic acid (FA). After washing with with 5% FA, C18-bound peptides were eluted with 80% AcN in 5% FA. Six fractions containing eluted peptides were dried in a SpeedVac concentrator SVC 100 (Savant Instruments Inc.). Peptides were dissolved in 200µl of 5% FA and their amounts were estimated using Nanodrop ND-1000 (Thermo Scientific). Peptides were dried again and stored at -20°C before TiO_2 enrichment.

Phosphopeptide enrichment

Each of 6 fractions was dissolved in 6% Trifluoroacetic acid (TFA), 80% AcN in a volume of 500-1000 µl depending on a peptide amount. Enrichment was performed with home-made tip-columns containing Sachtopore-NP TiO_2 beads (20 µm, 300 Å; ZirChrom, Anoka, MN) as described by Imanishi et al.[50] with small modifications. The ratio of the TiO_2 resin to peptides (in mg) was 1-4 to

1, with increased amounts of the resin used for hydrophilic fractions. TiO_2 tip-columns were built in water and activated with 6% TFA, 80% AcN. After loading of peptide samples, columns were washed twice with the same solution and once with 0.1% TFA. Phosphopeptides were eluted with 5% ammonia (NH_3) in water, and immediately FA was added to final concentration of 5%. The enriched peptides were desalted using microcolumns that were made with pieces of Empore C8 or C18 disks (3M, St. Paul, MN) packed into a 200-µl pipette tip. Enriched phosphopeptides originated from the tC2 cartridge were first loaded on C8 disks following by loading of flow through material on C18 disks; peptides from C8 and C18 cartridges were desalted on C18 disks. Washes and elution of bound peptides were performed as described by Imanishi et al.[50] Eventually, 9 peptide fractions were obtained for LC-MS/MS analysis in a single experiment. In total, three experiments were performed for both low-CO_2 and high-CO_2 grown cells.

Preparation of phosphopeptides for SRM analyses

Designed SRM assays were verified with phosphopeptides representing the whole phosphoproteome. After trypsin digestion of 4-5 mg of total protein performed as described above, peptides were acidified with FA to pH 2-3 and desalted using C18 cartridge (Waters, Sep-Pak Vac 3 cc, 500 mg). Peptides were eluted with 80% AcN in 5% FA and dried in a SpeedVac concentrator SVC 100 (Savant Instruments Inc.). Further, they were dissolved in 50µl of 5% FA and their amounts were estimated using Nanodrop ND-1000 (Thermo Scientific). Enrichment was performed as described above for data-dependent acquisition (DDA) samples using a 1:4 ratio of peptides to the TiO_2 resin. Phosphopeptides were desalted on C18 cartridges (Waters, Sep-Pak Vac 1 cc, 100 mg) prior to MS analysis.

LC−MS/MS Analysis

TiO_2-enriched peptides were analysed by LC-MS/MS using a Q Exactive™ Hybrid Quadrupole-Orbitrap mass spectrometer (Thermo Scientific) connected in-line with an Easy-nLC HPLC system (Thermo Scientific). Peptides were separated on a C18 pre-column (5 x 0.3 mm, PepMap C18, LC Packings) and a C18 nano-column (15 cm x 75 μm, Magic 5 μm200 Å C18, Michrom BioResources Inc., Sacramento, CA, USA) with a flow rate of 300 nL/min, using 0.1% FA, 2% AcN as a buffer A and 0.1% FA, 95% AcN as a buffer B. A 120-min gradient was applied: from 2% to 20% B in 70 min, from 20% to 40% B in 30 min, up to 100% B in 5 min followed by 100% B for 15 min. Mass spectrometer was equipped with an electrospray ionization source and was operated in the positive ion mode, with ionization voltage of 2300 V. An information-dependent MS data acquisition (DDA) was carried out using following parameters: MS survey scans were performed in a mass range of 300-2000 m/z with resolution of 17000, ten most intensive ions with charge state 2-4 were fragmented using a high energy collision dissociation (HCD) mode with the normalized collision energy (nCE) value of 30 eV, isolation window was 2.0 m/z, MS/MS ion scans were collected in a mass range of 100-2000 m/z with resolution of 17500, with a 20-sec dynamic exclusion of an ion for fragmentation.

Data Processing and Validation

The obtained data were primarily analysed using the in-house Mascot 2.4 (Matrix Science, London, UK) server via Proteome Discoverer 1.4 (ThermoFisher Scientific). A custom *Synechocystis* 6803 database applied for searches contained all predicted proteins of *Synechocystis* 6803 (genome- and plasmids-encoded) and was supplemented with a list of common laboratory contaminants; the FASTA file with sequences of *Synechocystis* 6803 proteins was downloaded from Cyanobase, http://genome.microbedb.jp/cyanobase/Synechocystis. Following search criteria were applied: digestion with trypsin, one missed cleavage allowed, precursor mass deviation tolerance of 10 ppm,

fragment mass tolerance of 0.02 Da, carbamidomethylation of Cys was set as a fixed modification whereas Met oxidation, acetylation for N-termini of proteins, and phosphorylation of S, T and Y were considered as variable modifications. A probability value for a primary Mascot search was 95%. Phosphopeptides identified in Mascot searches were further analysed with the Proteome Discoverer v. 1.4 and PhosphoRS v. 3.0[36] software. Peptides shorter that 6 amino acids, with peptide rank and search engine rank values higher than 1, or with a peptide score lower than 25 were filtered out. For assessment of an experimental false discovery rates, the custom *Synechocystis* 6803 database was appended by a list of decoy reverse *Synechocystis* proteins. In addition, a database of human proteins (SwissProt version 2014_08; Homo sapiens) was used to evaluate the amounts of false-positive matches that could be accidentally found in another, evolutionarily distant organism..

SRM analysis

A group of phosphopeptides originated from proteins participating in light-harvesting, photosynthesis and photosynthesis-related processes was further analysed using the SRM approach[51] in order to verify/improve assignments of phosphorylation sites and to build quantitative assays. The peptide spectral library was created from the data obtained by DDA LC-MS/MS as described above, and Q1/Q3 transitions were generated using Skyline software version 3.1.[52] Fragment ions providing information about localization of a phosphorylated amino acid residue were prioritised. A triple-stage quadrupole TSQ Vantage mass spectrometer (Thermo Scientific) connected in-line with an Easy-nLC HPLC system (Thermo Scientific) was used in SRM experiments. For verification of transitions, phosphopeptides spiked with Biognosys iRT synthetic peptides (Escher et al., 2012) as retention time standards were subjected to HPLC and MS. After desalting on a C18 pre-column (5 x 0.3 mm, PepMap C18, LC Packings), peptides were separated on a C18 nano-column (15 cm x 75 μm, Magic 5 μm200 Å C18, Michrom BioResources

Inc., Sacramento, CA, USA) using 0.1% FA as a buffer A and 0.1% FA, 80% AcN as a buffer B in a following 60-min gradient: from 5% to 26% B for 35 min, from 26% to 43% B for 15 min, 43% to 100% B for 2 min followed by 100% B for 10 min, with a flow rate of 300nL/min. The TSQ Vantage mass spectrometer was operated in the positive ion mode with a capillary temperature of 270 °C, spray voltage of +1600 V and collision gas pressure of 1.2 mTorr. Q1 and Q3 peak width (FWHM) parameters were set to 0.7 and cycle time to 2.5 s; minimal dwell time was 30 ms. The result raw files were imported into Skyline and SRM peak groups corresponding to phosphopeptides were manually selected using dotp values and the retention time information from DDA. In specific cases where phosphorylation site allocation remained uncertain, "heavy" peptides containing C-terminal K or R labeled with 13C(6)15N(2) or 13C(6)15N(4), respectively, were ordered from Thermo and analysed separately or spiked into the native samples.

RESULTS

To detect photosynthesis-related phosphoproteins, the cyanobacterium *Synechocystis* 6803 was subjected to the shotgun phosphoproteomic analysis.[53-56] Cells were grown in two environmental conditions, in air (0.04% CO_2) and in high CO_2 (3%), to diversify a proteome pattern and to increase possibilities to detect novel phosphopeptides. In order to avoid non-functional phosphorylation/dephosphorylation events during protein extraction, cells were broken in the denaturing conditions in the buffer containing inhibitors of proteinases, kinases and phosphatases. In addition, the detergent (DM) was added to the crude cell extract to ensure solubilisation of integral thylakoid membrane proteins involved in photosynthesis. After digestion of proteins with trypsin and peptide fractionation, phosphopeptide enrichment was performed using TiO_2[57,58] and followed by LC-MS/MS.

Data analysis was performed with the Proteome Discoverer software using the Mascot search engine. To optimize a Mascot peptide score cut-off value for identification of

phosphopeptides, searches were carried out against the custom database of *Synechocystis* proteins encoded by the genome and 7 plasmids which was supplemented with the corresponding reverse decoy database and the list of common laboratory contaminants including keratins (DB-SYN-REV-CON). Cut-off values of 15, 20, 25 and 30 for a Mascot peptide score were applied in searches followed by calculation of FDR values. Results are shown in the Supplemental Table S1 in the Supporting Information. We have selected 25 as a threshold for the peptide score cut-off value; that resulted in 1% FDR for phosphopeptides and 0.19% FDR for all detected peptides. Alternatively, the search was performed against the DB-HUM, the database of human proteins from the the NCBI selected with the taxonomy Homo sapience, which was supplemented with the same list of contaminants. The latter database was used to evaluate amounts of false-positives that could be erroneously found in an another organism which is evolutionarily distant from *Synechocystis* 6803. A search of our experimental data against DB-HUM with the chosen parameters produced identification of only two human phosphopeptides (Supplemental Table S1 in the Supporting Information). They represent true false-positive results since identical or highly homologous peptides do not exist in the *Synechocystis* 6803 proteome (based on the genome and plasmids' sequences). Thus, we have selected rather stringent filtering in the process of phosphopeptide recognition.

Localization of phosphorylation at a specific S, T or Y residue predicted by Mascot was further assessed with the PhosphoRS algorithm[36] included into the Proteome Discoverer software. Mascot results and PhosphoRS probabilities for every peptide spectral match (PSM) are shown in the Supplemental Table S2 in the Supporting Information. In total, we have identified 428 *Synechocystis* 6803 phosphopeptides, fifteen of them contained two phospho groups and one peptide was triply phosphorylated. Taking into account trypsin miscleavage events and Met oxidation, the list of phosphopeptides was condensed into 300 unique amino acid sequences from 190 proteins. In many cases, phosphopeptide isoforms were discovered for the same amino acid

sequence. In total, we discovered 367 phosphorylation sites, and for 287 of them a position of a phosphorylated residue was identified with 99-100% probability. The value was slightly lower (75-99%) for 16 phosphorylation sites; in other cases, the probability values were below 75% and, therefore, exact locations of modification in this group of phosphopeptides remained uncertain. The distribution of pS, pT and pY in peptides with known modification sites (with a probability > 75%) was calculated to be 61/34/5%, respectively, which resembles the one found in human, higher plant and some bacteria[12,14,54,59-61]. Spectra of detected phosphopeptides are shown in the Supplemental Figure S1 in the Supporting information.

Although the majority of peptides were singly phosphorylated, often several phosphopeptides originated from the same protein. About 28% of discovered phosphoproteins produced two or more phosphopeptides. For example, many PBS components belong to this group including both subunits of phycocyanin (Sll1578, Sll1577) and allophycocyanin (Slr2067, Slr1986). As a maximum, 12 unique trypsin-generated peptide sequences that contained pS or pT residues were found in the CcmM protein (Sll1031) which is involved in the biogenesis of carboxysomes.[62] Among other multiply phosphorylated proteins were fructose-bisphosphate aldolase class II (Sll0118), unknown Sll0103 protein, the bicarbonate transporter SbtA (Slr1512) and some proteins involved in regulatory functions in *Synechocystis* 6803.

Considering amount of spectral counts that roughly indicate abundance of a peptide in the samples,[63,64] rather limited group of peptides was phosphorylated in substantial amounts. The PII regulatory protein (Ssl0707), anti-sigma factor antagonists (Slr1859; Ssr1600; Ssr1600), phycocyanin and allophycocyanin subunits, the CcmM protein, phosphoglucomutase (Sll0726), the AbrB-like transcriptional regulator Sll0822[65] and the unknown Slr0148 protein yielded the most abundant phosphopeptides in our experiment. In contrast, about 38% of phosphopeptides were registered only once (Supplemental Table S2 in the Supporting Information)

Classification of phosphoproteins in *Synechocystis* 6803

Phosphoproteins of *Synechocystis* 6803 detected by LC-MS/MS and their functional distribution are presented in Figure 2 and Supplemental Table S3 in the Supporting Information. Identified phosphoproteins participate in various intracellular processes that are important for cell survival and acclimation to environmental conditions.

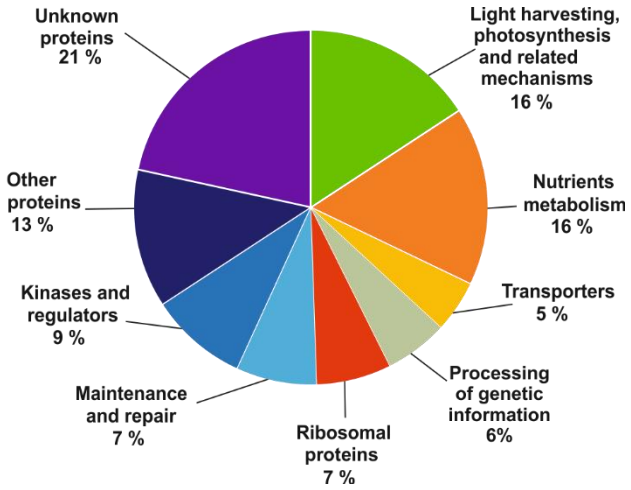

Figure 2: Pie chart representations of the functional distribution of phosphoproteins detected by LC-MS/MS**.**

One of the largest groups comprised phosphorylated proteins involved in light harvesting, photosynthesis and carbon fixation (Figures 1, 2). Among PBS components, in addition to multiply phosphorylated phycocyanin and allophycocyanin that constitute disk-shaped modules of rods and the core, respectively, this PTM was detected in linker polypeptides CpcC2 (Sll1579, L_R^{30}), CpcD (Ssl3093, L_R^{10}), ApcC (Ssr3383, L_C) and CpcG1 (Slr2051, L_{RC}) that stabilize the bulky PBS structure and optimize transfer of excitation energy from the peripheral rods to the PBS core.[66] Phosphorylation was observed also in the core-membrane linker polypeptide ApcE (Slr0335, L_{CM}) which is important for the attachment of PBS to the thylakoid membrane and transfer of excitation energy from the PBS core to the photosynthetic reaction center. In the photosynthetic machinery, phosphorylation was detected in several subunits of PSI, PSII and Cyt b_6f complexes including, for

example, PsaD (Slr0737) that binds ferredoxin, and PsaL (Slr1655) which is important for the formation of the PSI trimer.[67] We specifically note that PsbA the D1 protein of the PSII complex was discovered in a phosphorylated form. LC-MS/MS analysis of the most hydrophilic fraction of the *Synechocystis* 6803 phosphoproteome revealed that phosphorylation of the N-terminal peptide Ac-TTTLQQR may occur at any of three T residues. The corresponding spectra together with the one of the non-phosphorylated form are shown in Figure 3.

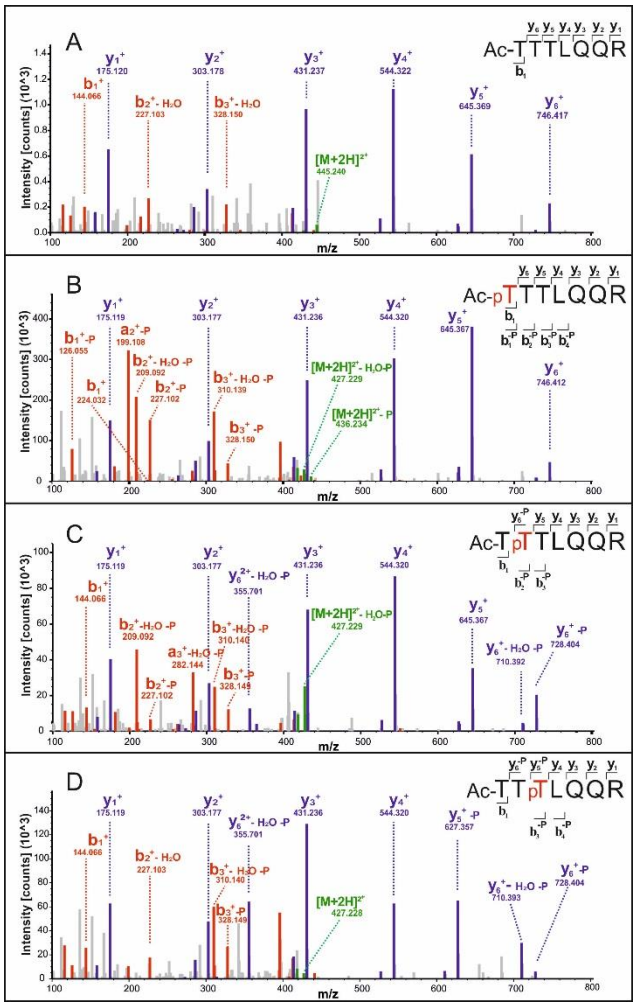

Figure 3: Individual spectra for Ac-TTTLQQR, the N-terminal peptide of the PSII D1 protein. (A) non-phosphorylated peptide, (B-D) three phosphopeptide isoforms.

Further, subunits of ATP synthase which is driven by the trans-membrane proton gradient resulting from electron transfer and concomitant pumping of proton to the lumen also appeared to be phosphorylated, as well as FNR (Slr1643) that finalizes conversion of light energy into NADPH. In addition, phosphopeptides were found in the orange carotenoid protein (OCP, Slr1963), flavodiiron proteins Flv2 (Sll0219) and Flv3 (Sll0550) which are involved in photoprotection mechanisms, and both subunits of Rubisco (RbcL, Slr0009 and RbcS, Sll0012) that performs the photosynthetic CO_2 fixation.

Another large group of phosphoproteins was composed of enzymes participating in metabolism of nutrients. Many phosphorylated enzymes were found in interconnected pathways of carbon metabolism, namely in glycolysis, the pentose phosphate pathway and in the Calvin-Benson-Bassham cycle at the stages important for regeneration of Rubisco. Some phosphoproteins were engaged in other pathways of carbon metabolism, *e.g*. biosynthesis of carbohydrates, lipids, glycans, and secondary metabolites, as well as in the biogenesis of carboxysomes, like the CcmM protein (Sll1031) which is crucial for Rubisco aggregation and initiation of carboxysome formation.[62,68] Several phosphoproteins were involved in nitrogen metabolism including the PII protein (Ssl0707), the central regulator of the carbon-nitrogen balance; two enzymes with glutamine synthetase activity, GlnA (Slr1756) and GlnN (Slr0288); and cyanophycin synthetase (Slr2002). In addition, phosphorylation was observed in ferredoxin-sulfite reductase Sir (Slr0963) that contributes to the metabolism of sulphur. Further, a group of phosphoproteins was involved in transport of nutrients and other compounds, like SbtA (Slr1512), the Na-dependent bicarbonate transporter; Amt1 (Sll0108), the ammonium/methylammonium permease, *etc*.

Phosphoproteins were discovered in systems responsible for processing of the genetic information including basic elements of transcription (Sll1789 and Ssl2982, subunits of RNA polymerase) and translation (Sll1099, the Tu elongation factor and Slr0744, the IF-2 translation initiation factor) machineries. It is important to note a group of phosphoproteins participating in a

regulation of gene expression, like anti-sigma F factor antagonists Slr1856, Slr1859 and Ssr1600; KaiC (Slr1942), the component of circadian clock; Fur (Sll0567), the transcription factor that regulates many genes involved in iron homeostasis and oxidative stress response; LexA (Sll1626) controlling genes in the varied regulatory networks, and CyAbrB (Sll0359), one of two AbrB-like transcriptional regulators in *Synechocystis* 6803. Phosphorylation was observed in proteins involved in maintenance and repair, in particular in chromosome partitioning, DNA replication and repair, RNA folding and degradation, protein folding (GroEL1 and GroEL2) and secretion. Several ribosomal proteins, from both large and small subunits, also contained phosphorylated residues.

Many phosphoproteins participate in regulation and signal transduction, similarly to other organisms. Several protein kinases, namely SpkB (Slr1697), SpkC (Slr0599), SpkD (Sll0776), SpkF (Slr1225), SpkG (Slr0152) and probable phosphatase Sll1033 that perform reversible O-phosphorylation were found to be modified. It is important to note two-component sensor histidine kinases and response regulators like Hik12, Hik21, Hik36, Hik43), Crr23, Crr43, *etc* that appear to undergo O-phosphorylation beside functionally important modifications on H/D residues. In addition, phosphoproteins were found among components of signal transduction important for pili biogenesis (McpA, Slr1044) and phototaxis (PixH, Sll0039 and PixI, Sll0040).

Among other enzymes that were found in a phosphorylated form are those involved in biosynthesis of amino acids, nucleotide metabolism, tRNA biogenesis, metabolism of cofactors and vitamins. However, functions of many detected phosphoproteins remain at present unknown. One of them is the Slr0148 protein which is similar to ferredoxin. Its gene belongs to the *slr0144-slr0152* gene cluster that constitutes the PAP (Photosystem II assembly proteins) operon shown to be involved in increasing photosynthetic efficiency.[69] In total, hypothetical and uncharacterized phosphoproteins contribute about a quarter of discovered phosphoproteome of *Synechocystis* 6803.

Design of the SRM library for assessment of phosphorylation events in *Synechocystis* 6803 proteins involved in light harvesting, photosynthesis and photosynthesis-related processes

LC-MS/MS analysis of fractionated *Synechocystis* 6803 phosphoproteome indicated the occurrence of about 100 phosphorylation sites in proteins associated with the capture of light, photosynthetic electron transfer, photoprotection and carbon fixation suggesting that phosphorylation may play an important role in regulation of photosynthetic performance in cyanobacterial cells, similarly to the mechanisms discovered in plants.[39,70-73] After manual inspection of spectra, we set the following goals: i) to confirm phosphorylation site assignments suggested by PhosphoRS algorithm with a probability value > 75%, ii) to identify phosphorylation sites in phosphopeptides where assignment was uncertain, iii) to evaluate possibilities for assessment of individual phosphopeptides isomers, and iv) to setup quantitation assays for phosphorylation events. At this step, we exploited the SRM approach.[41,42,51] In this method, the phosphorylated precursor was targeted with Q1 *m*/*z* values while groups of co-eluting transitions (Q1/Q3) helped to pinpoint modification sites. The data obtained by DDA LC-MS/MS were used to create the peptide spectra library and to design transitions. The spectra were acquired on a Q Exactive instrument with the HCD fragmentation mode which generates fragments with similar type and intensity that the ones in TSQ Vantage[74] used for SRM. Specific fragment ions characterizing positions of phosphorylation sites were prioritized; besides y and y-98 fragment ions, b and b-98 were also used where they were beneficial for the site localization. Alternative isoforms were predicted for phosphopeptides with multiple potential modification sites where probability of the localization of the modified residue was < 99%. Originally, transitions were tested on TiO_2-enriched fractionated *Synechocystis* 6803 samples prepared for DDA LC-MS/MS and spiked with iRT peptides; examples of these tests are presented in the Skyline file 3 in the Supporting information. For peptides observed in both doubly and triply charged states, the more

intensive precursors were chosen. Up to 15 fragment ions for a peptide were originally examined; later, we selected the most representative sets of transitions for each phosphopeptide or phosphopeptide isoform. In several cases when chromatographic resolution of phosphopeptide isomers remained problematic, corresponding "heavy" peptides were synthetized and subjected to SRM (Supplemental Table S4 and Skyline file 1 in Supporting information) to corroborate the characteristic transitions and retention time values. Later, consolidated transition sets were verified with TiO_2-enriched unfractionated *Synechocystis* 6803 samples representing the total phosphoproteome spiked with iRT markers and "heavy" peptides. Some fragment ions were omitted at that step due to interferences coming from closely eluting abundant native peptides. Finally, the spectral library and the comprehensive set of intensive transitions with those pinpointing a phosphorylation site (Supplemental Table S5) were merged with retention time index values (Skyline file 2 in Supporting information). The Skyline files with designed isomer-specific transitions and acquired data for native samples and synthetic peptides were submitted to Panorama, https://panoramaweb.org

The phosphorylation sites verified with the SRM approach are presented in Table 1. The corresponding proteins representing PBS components, subunits of PSI, PSII, and Rubisco, as well as elements of photoprotection and acclimation mechanisms are depicted in Figure 1. Five peptides, ANHGLpSGDAR (CpcA), VVpSQADAR (CpcB), pSIVNADAEAR, AFVpTGGAAR (ApcA), and FVELGQVpSAIR (ApcE), contained unique phosphorylation sites. The phosphorylation events in these peptides were confirmed with SRM transitions. For phosphopeptides from phycocyanin and allophycocyanin, intensities of fragment ions were rather prominent, most probably reflecting a high abundance of the PBS rod proteins in the total protein content.

Other peptides contained multiple potential phosphorylation sites in their sequences. In some of them, only a single isoform was predicted by both Mascot and PhosphoRS for all the Peptide Spectral Matches (PSMs) in DDA LC-MS/MS despite of existence of other potential sites.

The SRM analysis confirmed those results. For pSGILYPVIVR (PsaE), the pS^{1} position was verified by transitions corresponding to $y5^{+;}$ $y6^{+}$, $y7^{+}$, $(p)b3^{+}$ and $(p)b3^{+}$-98 fragment ions. Other examples are the pS^{3} position in Ac-AEpSNQVVQAYNGDPFVGHLSTPISDSAFTR (PsaL), the pS^{5} site in EVTApSLVGADAGK (ApcB), pS^{1} in pSFQVYR (Cpc2), pT^{1} in pTFQGPPHGITVER (RbcL), pS^{1} in pSENPNCYIR (RbcS) and pS^{1} in pSEELQPNQTPVQEDPK (HliD). For some phosphopeptides, isoforms were predicted by Mascot and/or PhosphoRS in different PSMs; however, we succeeded to validate by SRM only a single form. For the phosphorylated SYFASGELR peptide from ApcB, pS^{1} and pS^{5} were suggested by Mascot and pRS but only S^{1} was verified with intensive $y5^{+}$- $y7^{+}$ fragment ions discriminating pS^{1} against pS^{5}. In addition, $(p)b3^{+}$-98 indicated pS^{1} and not pY^{2} since pY residues do not loose phosphoric acid in CID/HCD fragmentation.[32,75] From suggested pT^{5} and pS^{11} in phosphorylated VAIETNDNLLSGLLGQDLR (Slr0148), the pT^{5} position was supported by intensive $y9^{+}$ and $y10^{+}$ fragment ions, both for the doubly and triply charged precursor. In TLEVIpTTHNR (Slr0148), only pT^{6} was found to be phosphorylated. It was confirmed by strong $y4^{+}$ and $(p)y5^{+}$-98 fragment ions while no $(p)y4^{+}$-98 or non-phosphorylated $y5^{+}$ - $y8^{+}$ signals were detected in SRM with the Q1 value set for the phosphopeptide. Further, in doubly charged GEYLSGpSQLDALSATVAEGNKR (CpcB), strong $y12^{+}$, $y13^{+}$ and $(p)y17^{+}$-98, $(p)y18^{+}$-98 fragment ions unambiguously specified the pS^{7} position as the modification site in DDA LC-MS/MS. However, the *m*/*z* values for last two ions (1698.877 and 1785.909, respectively) were out of the acquisition range of the TSQ mass spectrometer. Instead, we selected more intense triply charged precursor for the SRM library where $[(p)y17\text{-}98]^{2+}$ and $[(p)y18\text{-}98]^{2+}$ fragment ions together with $y10^{+}$, $y11^{+}$ and $b5^{+}$ were used for confirmation of the pS^{7} site. We did not discriminate by SRM another isoform, pS^{5}. In phosphorylated IAETLTGpSR (ApcA), the pS^{8} modification site was clearly determined with the series of $(p)y3^{+}$-98 - $(p)y8^{+}$-98.

The next group comprised phosphopeptides predicted by Mascot/PhosphoRS and detected by SRM in several isoforms. For some peptides, the isoforms were well resolved in time during

HPLC and intensities of characteristic fragment ions were good enough to unambiguously localize modification sites using the native samples. The example is shown in Figure 4. The pS^{10} and pS^{6} isomers of ITGNASAIVSNAAR from CpcB with iRT values 16,77 and 23,79, respectively, eluted with about 2-min interval. Both isoforms were unambiguously differentiated with characteristic fragments $(p)y5^{+}$-98, $(p)y6^{+}$-98, $(p)y8^{+}$-98 for the pS^{10} and $y5^{+}$-$y8^{+}$ for the pS^{6}.

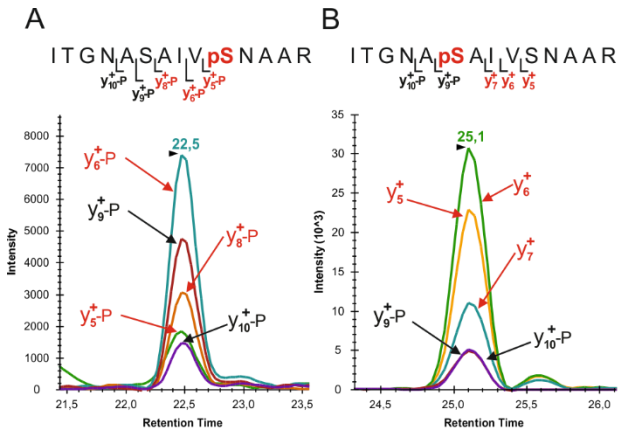

Figure 4: SRM spectra of pS^{7} (A) and pS^{4} (B) isoforms of the phosphopeptide. ITGNASAIVSNAAR (CpcB). Isoforms resolved well during HPLC eluting at 22,5 min and 25,1 min, respectively. Common fragment ions for the two forms are shown in black, while the characteristic fragment ions unambiguously localizing modification sites are in red. Retention time values are shown in green

Similarly, pS^{1} and pT^{8} isomers of SINPAANTIPK from CpcG1 were well resolved during HPLC and characterized with intensive $y8^{+}$ and $(p)b3^{+}$-98 characteristic ions for the pS^{1} form and $(p)y4^{+}$-98, $(p)5^{+}$-98, $(p)y6^{+}$ as the most intensive transitions for the pT^{8} form. The largest time difference was observed for two phosphorylated forms of SLGTPIEAVAQSVR from ApcA, pS^{1} and pS^{12}. These two phosphopeptides which did not have common transitions in our SRM library due to distal positions of modified residues in the peptide sequence eluted with about 9-min difference in our 60-min SRM run. For certainty, we confirmed the identities of both isoforms and

corresponding iRT values with "heavy" synthetic peptides (Skyline file 1 in the Supporting information). Further, in FGGSTGGLLSK from PsaD, all three originally detected phosphorylation sites, pS^4, pT^5 and pS^{10}, were validated by SRM (Skyline file 2 in the Supporting information). The three isoforms eluted closely to each other. The pT^5 form that eluted first was resolved rather well while following pS^{10} and pS^4 variants slightly overlapped, with (p)$y8^+$-98, (p)$y9^+$-98 and (p)$y10^+$-98 fragment ions common for all three forms. For pT^5, characteristic fragment ions $y6^+$ and (p)$y7^+$-98 were the most intense in the peak. The pS^4 position was revealed by transitions with the mass of the non-modified $y7^+$ ion while (p)$y3^+$-98 and (p)$y6^+$-98 clarified the pS^{10} position. Fragment ions and iRT values were confirmed with "heavy" analogues. Similarly, three isomers at T^1, S^8 and S^{12} for TPLTEAVSTADSQGR from CpcA were resolved in time during HPLC. The pT^1 variant was uniquely characterized with the $y9^+$-$y12^+$ ions while pS^8 and pS^{12} isoforms could be distinguished by $y4^+$, $y5^+$ and $y6^+$ fragment ions or the corresponding phosphorylated fragment ions with the neutral loss of 98 Da, respectively. Next, the three D1 phosphopeptides, Ac-pTTTLQQR (pT^1), Ac-TpTTLQQR (pT^2) and Ac-pTTpTLQQR (pT^3) were well resolved in time upon elution from the C18 column and confirmed by specific transitions for endogenous peptides and co-elution with their "heavy" counterparts. The positions of modification sites were differentiated with $y5^+$ and $y6^+$ for pT^1, $y5^+$ and (p)$y6^+$-98 for pT^2, (p)$y5^+$-98 and (p)$y6^+$ for pT^3; b-ions were excluded due to a strong interference from other peptides in complex mixtures. In native fractionated samples, the three isoforms were intensive and clearly resolved in the most hydrophilic fraction (Skyline file 3 in the Supporting information) but in the samples with unfractionated phosphopeptides the intensities of SRM transitions were low; therefore, spiking with "heavy" analogues was beneficial. Similarly, "heavy" analogues helped to differentiate resolved pT^1 and pS^4 isoforms of the phosphorylated TELSGQPPK peptide of PsaD with low intensities in non-fractionated samples. Transitions containing masses of $y6^+$ - $y8^+$ and (p)$b3^+$-98 confirmed pT^1 while (p)$y6^+$, (p)$y7^+$, (p)$y6^+$-98, (p)$y7^+$-98 and $b2^+$ corroborated pS^4.

Two distinct phosphopeptides that belong to the same group are pSKNFLNTTNDPNSGK (pS^{1}) from PsaF and IGQNPEPVTIKFpSGK (pS^{13}) from PsaD. They are products of trypsin miscleavage and, therefore, are poorly suited for quantitation purposes. Both phosphorylation sites could be targeted only in the partially digested form (or by using another cleavage agent) since in the fully cleaved forms they were too short for analysis. However, the SRM approach was useful for validation purposes. Triply charged precursors were used to set Q1 values for both phosphopeptides. The pS^{1} form of the former phosphopeptide was confirmed with transitions containing masses of $y3^{+}$, $y5^{+}$ (most intensive), $y7^{+}$, $y8^{+}$, $y9^{2+}$ and $y12^{2+}$ fragment ions. In the latter one, pS^{13} was distinguished with the transition corresponding to the rather intensive characteristic $y4^{+}$-98 fragment ion; phosphorylation of T^{9} in this sequence or in fully cleaved IGQNPEPVT has not been detected.

Besides validation of DDA LC-MS/MS results, the SRM approach revealed occurrence of novel phosphorylation sites. In addition to the pT^{1} isoform of TFDLSPSWYVEALK (CpcA) detected in LC-MS/MS, SRM showed the existence of the pS^{7} variant. The common fragment ions $y6^{+}$ and $y7^{+}$ for the two forms partially overlapped on the chromatogram (Figure 5). The transitions corresponding to $y9^{+}$ - $y11^{+}$ and (p)$b3^{+}$-98 fragment ions validated the pT^{1} isoform while the ones corresponding to (p)y10-98^{+}, (p)$y9^{+}$, (p)y9-98^{+}, $b3^{+}$ fragment ions substantiated the S^{7} phosphorylation site which was not detected originally. The characteristic ions could be used for quantitation of these individual isoforms.

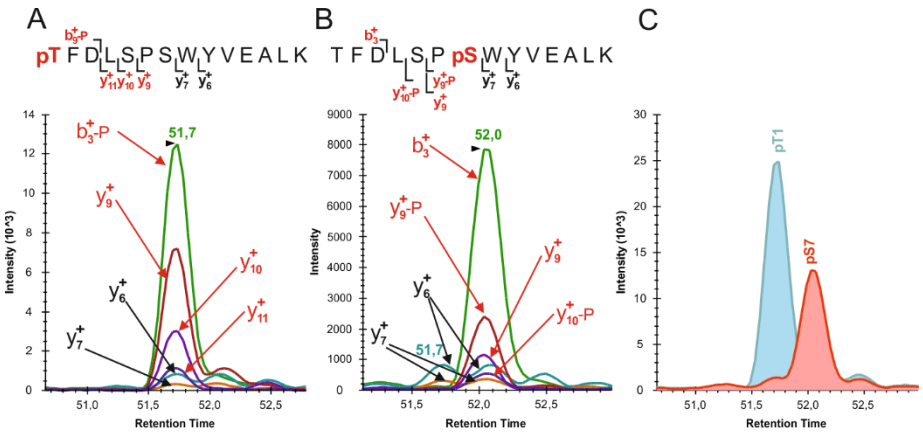

Figure 5: SRM spectra of two phosphopeptide isoforms of the TFDLSPSWYVEALK (CpcA). (A) The pT^{1} isoform identified by LC-MS/MS and confirmed by SRM. (B) The pS^{7} isoform revealed by SRM. Common fragment ions for the two forms are shown in black while the characteristic fragment ions are in red. Retention time values are shown in green. (C) Partial overlapping of the two phosphopeptides.

In another peptide, TSLVSAQR of CpcC2, where three modification sites are available, only pT^{1} was identified in DDA LC-MS/MS. This phosphorylation site was confirmed by SRM with $(p)b3^{+}$, $(p)b3^{+}$-98, $y5^{+}$, $y6^{+}$ and $y7^{+}$ fragment ions. In addition, SRM helped to discover another isoform, pS^{5}, which eluted later than pT^{1}; it was identified with transitions corresponding to $(p)y5^{+}$-98 and $(p)y6^{+}$-98. To verify, we analyzed "heavy" analogues of pT^{1}, pS^{5} and probable pS^{2} isoforms. Results confirmed occurrence of T^{1} and S^{5} isoforms and their iRT values. Moreover, it appeared that pT^{1} and pS^{2} "heavy" peptides co-eluted, and intensities of transitions corresponding to the $(p)y7^{+}$ and $(p)y7^{+}$-98 ions in the pS^{2} isoform were too low to distinguish it from pT^{1} (Skyline file 1 in the Supporting information). Therefore, the occurrence of the pS^{2} isoform in native samples could not be excluded.

The SRM technique combined with application of "heavy" peptides was especially beneficial in investigation of phosphorylation in QPALVGASSDSR from ApcE,

IAEPVVPPQDTASR from OCP, and SLDSDLEK from Flv3. In the phosphorylated QPALVGASSDSR peptide of ApcE, the modification site was uncertain in DDA LC-MS/MS. In several spectra, pS^{8} was identified by both Mascot and PhosphoRS with the probability > 99% while in other spectra results differed. Mascot suggested that all three sites, S^{8}, S^{9} and S^{11}, could be phosphorylated, while PhosphoRS predicted zero probability for modification at S^{11}. SRM analysis of "heavy" peptides corresponding to pS^{8}, pS^{9} and pS^{11} isoforms demonstrated that they fully co-eluted during HPLC (Skyline file 1 in the Supporting information); moreover, intensities of the characteristic ions $(p)y4^{+}$ and $(p)y4^{+}$-98 were too low to differentiate pS^{8} and pS^{9}. SRM analysis of fractionated native samples (Skyline file 3 in the Supporting information) revealed the presence of rather intensive non-modified $y2^{+}$ fragment ion in the transition group supporting pS^{8}/pS^{9}. Thus, pinpointing location of the phosphorylation site in this phosphopeptide remained to be difficult; however, phosphorylated QPALVGASSDSR could be targeted with common fragment ions keeping in mind uncertainty of the modification site at S^{8}:S^{9}:S^{11}. Next, the IAEPVVPPQDTASR phosphopeptide from OCP was discovered in DDA LC-MS/MS as a single PSM, and the pT^{11} modification site was predicted by both Mascot and PhosphoRS. However, in SRM of native samples, transitions corresponding to $(p)y8^{+}$, $(p)y8^{+}$-98 and $(p)y7^{+}$-98 showed two poorly resolved tailing peaks indicating a possibility for another phosphorylation site. "Heavy" analogues of the pT^{11} and potential pS^{13} isoforms demonstrated a similar tailing of peaks and the same iRT values (Skyline file 1 in the Supporting information). Despite the characteristic fragment ions, $y2^{+}$ and $y3^{+}$, or $y2^{+}$-98 and $y3^{+}$-98, respectively, were not prominent enough to differentiate the two forms, analysis of native samples spiked with "heavy" peptides suggested that phosphorylation most probably occurred at both T^{11} and S^{13} positions. Finally, we investigated a phosphorylated SLDSDLEK peptide from Flv3 for which two forms, pS^{1} and pS^{4}, were identified in DDA LC-MS/MS. In SRM, amounts of these two phosphopeptides appeared to be low in total

phosphoproteome samples. Therefore, application of "heavy" peptides was necessary to optimize transitions for the two isoforms and to estimate their iRT values for future quantitation studies.

Technical variations of investigated transitions were calculated separately for samples from LC- and HC-grown cells (Supplemental Table S6 in the Supporting Information). The average coefficient of variation (CV) value for all transitions was about 21%. For few phosphopeptides, intensities of the transition groups varied depending, apparently, on growth conditions. The examples are pTFQGPPHGITVER and pSENPNCYIR from RbcL and RbcS, respectively. These cases indicated that experimentally observed intensities of the transition groups were indeed sample-dependent and showed that described SRM assays were applicable for future quantitation studies.

DISCUSSION

Investigations of O-phosphorylation in cyanobacteria were stimulated greatly by development of proteomic techniques and, in particular, by phosphopeptide enrichment methods.[27-31] The most extensive studies based on DDA LC-MS/MS analyses of pre-fractionated and enriched cyanobacterial phosphopeptides resulted in hundreds of detected phosphorylation sites in *Synechocystis* 6803[30,31] and *Synechococcus* 7002.[29] Moreover, Chen and coworkers[31] carried out site-directed mutagenesis of four phosphorylation sites in CpcB, the beta subunit of phycocyanin, and demonstrated that mutations affected energy transfer and state transition of photosynthesis in *Synechocystis* 6803. Spät et al.[30] examined the dynamics of *Synechocystis* 6803 (phospho)proteome in a response to nitrogen starvation. It is evident that along with searches for novel phosphoproteins, studies aiming to clarify biological roles of O-phosphorylation in cyanobacteria will expand in the nearest future. Quantitation of phosphorylation events that occur in cells exposed to challenging environmental conditions is a promising approach to pursue this goal. It, however, requires reliable, sensitive and straightforward methods that could be implemented in a relatively

simple manner to multiple samples. Spät and colleagues[30] quantified dynamics of 148 phosphorylation events using the chemical stable isotope labeling based on dimethylation of peptides. This quantitative experiment was based on DDA LC-MS/MS approach which is known to be biased towards abundant proteins and lacks reproducibility and precision in protein detection. An alternative and perspective approach is SRM which is capable to quantify selected proteins/peptides in complex samples consistently, reproducibly and with a high precision.[51] Due to a measurement of Q1/Q3 transitions, the method shows a greater sensitivity to peptides present in trace amounts which is important for analysis of phosphopeptides that are usually present in substoichiometric amounts to their unmodified counterparts. Application of the SRM technique for the targeted analysis of a phosphorylation network has been demonstrated.[76] Also, in contrast to dimethylation with stable isotopes, the method allows measurements across multiple samples.

We focused on phosphoproteins of *Synechocystis* 6803 that are involved in photosynthesis and photosynthesis-related processes in order to assign precisely the phosphorylation events that may be important in regulation of their efficiency. First, we performed the phosphoproteome analysis of *Synechocystis* 6803 cells grown in air (LC) and in 3% CO_2 (HC) using TiO_2 enrichment of phosphopeptides followed by LC-MS/MS analysis in the DDA mode. In HC conditions, CO_2 concentration around Rubisco is high enough to stimulate the efficient carbon fixation which necessitates increased demands for reducing equivalents and ATP resulting from photosynthesis. When cells are grown in air, external CO_2 concentration is low, photosynthesis rate decreases compared to HC conditions, and various carbon concentrating systems and photosynthesis-protection mechanisms become induced.[77-79] By using two different growth conditions, we aimed merely at enhancing the possibility to discover as many phosphorylated sites as possible; we did not attempt to compare the phosphoproteomes of HC- and LC-grown cells in the present paper. Similarly to other studies,[29-31] we pre-fractionated peptides prior to the TiO_2 enrichment to decrease a complexity of peptide mixtures in DDA LC-MS/MS. At this step, we identified 428 peptides

containing phosphorylated S/T/Y residues (Supplemental Table S2 in the Supporting Information), with the FDR value for phosphopeptides of 1% (Supplemental Table S1 in the Supporting Information). They corresponded to 367 phosphorylation sites in 190 proteins participating in various cellular functions (Figure 2 and Supplemental Table S3 in the Supporting Information).

Further, we concentrated on phosphoproteins involved in light harvesting, photosynthetic electron flow, carbon fixation and other photosynthesis-related processes like photoprotection, alternative electron flows and acclimation to light extremes. This group comprised about 90 phosphorylation sites which were detected by DDA LC-MS/MS in components of the PBS antenna, PSI and PSII subunits, Rubisco, OCP and flavodiironproteins that are involved in photoprotection and safeguarding of the photosynthesis machinery, and two poorly studied proteins, HliD and Slr0148 implicated in the light acclimation. Considering our selected protein set, comparison of our results with those of Spät et al.[30] and Chen et al.[31] revealed that some of phosphorylation sites were recognized in all three studies (Supplemental Table S7 in the Supporting Information); for example, pT^{3}, pS^{10} and pS^{14} in CpcA, one the PBS rod subunits that are highly abundant in cyanobacterial cells. In less abundant proteins, like PBS linkers, the detected phosphorylation pattern differed among studies (Supplemental Table S7 in the Supporting Information), most probably, due to differences in growth conditions, variations in sample preparation procedures, used analytical methods, etc. Thus, each study contributed to the common knowledge by revealing novel phosphorylation sites.

Investigation of a biological role of a specific protein phosphorylation event requires confidence in its identification. Therefore, we assessed the discovered phosphopeptides with the SRM approach which is highly selective and specific due to acquisition of Q1/Q3 (precursor/product) ion transitions.[51] The proteins comprising the SRM-verified phosphorylation sites are shown in red in Figure 1. Forty-five phosphorylation sites from the proteins of interest were distinguished by SRM with sets of co-eluting transitions comprising those unambiguously

proving positions of modified residues (Table 1). When necessary, synthetic "heavy" peptides were applied to distinguish phosphopeptide isoforms.

Table 1: List of phosphopeptides and phosphopeptide isoforms distinguished by SRM

Phosphopeptide	Phosphorylation site in		Heavy	iRT	Ions /
	peptide	protein[(a)]		Value	**Characteristic ions**
phycocyanin alpha subunit CpcA, Sll1578					
TPLTEAVSTADSQGR	pS[12]	14_S		29,28	**(y4$^+$, y7$^+$-y10$^+$, y12)$^+$-98**
TPLTEAVSTADSQGR	pS[8]	10_S		37,09	**y4$^+$-y7$^+$, (y8$^+$-y10$^+$)-98**
TPLTEAVSTADSQGR	pT[1]	3_T		41,85	**y4$^+$, y8$^+$, y9$^+$, y12$^+$**
TFDLSPSWYVEALK	pT[1]	121_T		101,66	y6$^+$, **y(9-11)$^+$, b3$^+$-98**
TFDLSPSWYVEALK	pS[7]	125_S		102,64	y6$^+$, **(y9$^+$-y10$^+$)-98, y9$^+$, b3$^+$**
ANHGLSGDAR	pS[6]	143_S		-29,90	y2$^+$, (y6$^+$-y8$^+$)-98
phycocyanin beta subunit CpcB, Sll1577					
ITGNASAIVSNAAR	pS[10]	53_S		16,77	**(y5$^+$-y6$^+$,y8$^+$)-98**, (y9$^+$-y10$^+$)-98
ITGNASAIVSNAAR	pS[6]	49_S		23,79	**y5$^+$-y8$^+$**, (y9$^+$-y10$^+$)-98
GEYLSGSQLDALSATVAEG NKR	pS[7]	22_S		76,84	**y9$^+$-y11$^+$**, (y16^{2+}-y18^{2+})-98, **b5$^+$**
VVSQADAR	pS[3]	10_S		-28,08	y4$^+$-y5$^+$, (y6$^+$-y7$^+$)-98
allophycocyanin alpha subunit ApcA, Slr2067					
SLGTPIEAVAQSVR	pS[12]	129_S	**x**	49,17	**(y5$^+$, y7$^+$-y8$^+$, y10$^+$)-98,y10$^+$**
SLGTPIEAVAQSVR	pS[1]	118_S	**x**	82,82	**y7$^+$-y8$^+$, y10$^+$, b3$^+$-98**
SIVNADAEAR	pS[1]	7_S		-9,02	y5$^+$-y8$^+$, b3$^+$-98
IAETLTGSR	pS[8]	46_S		-3,81	**y3-98**, (y5$^+$,y7$^+$-y8$^+$)-98
AFVTGGAAR	pT[4]	31_T		-5,58	y5$^+$, (y6$^+$-y7$^+$-y8^{2+})-98
allophycocyanin beta subunit ApcB, Slr1986					
SYFASGELR	pS[1]	29_S		32,76	**y5$^+$-y7$^+$, b3$^+$-98**
EVTASLVGADAGK	pS[5]	139_S		17,33	**y6$^+$, y8$^+$, (y9$^+$, y10$^+$)-98**, y11$^+$-98
phycobilisome rod linker polypeptide LR30, CpcC2, Sll1579					

SFQVYR	pS[1]	168_S		17,15	**y2^{+}-y5^{+}**
TSLVSAQR	pT[1]	2_T	**x**	-15,68	**y5^{+}-y7^{+}, b3^{+}-98**
TSLVSAQR	pS[5]	6_S	**x**	-9,44	**y4^{+}, (y5^{+}-y6^{+})-98**
phycobilisome rod-core linker polypeptide LRC, CpcG1, Slr2051					
SINPAANTIPK	pS[1]	224_S		16,92	**y6^{+},y8^{+}-y9^{+}, y8^{2+}, b3^{+}-98**
SINPAANTIPK	pT[8]	231_T		23,35	**(y4^{+}-y5^{+}, y7^{2+})-98, (y6^{+},y9^{+})**
phycobilisome core-membrane linker polypeptide LCM, ApcE, Slr0335					
FVELGQVSAIR	pS[8]	698_S		61,72	(y5^{+}, y7^{+}-y9^{+})-98
QPALVGASSDSR		99_S			
QPALVGASSDSR	pS[8]:pS[9]:pS[11]	100_S	**x**	-8,65	y(y5^{+}, y7^{+}), (y7^{+}-y8^{+})-98
QPALVGASSDSR		102_S			
photosystem II D1 protein, PsbA, Slr1311					
TTTLQQRFI	N-Ac-pT[3]	4_T	**x**	-16,03	y3^{+}-y4^{+}, **y5^{+}-98, y6^{+}**
TTTLQQR	N-Ac-pT[1]	2_T	**x**	-12,36	y3^{+}-y4^{+}**-y5^{+}-y6^{+}**
TTTLQQR	N-Ac-pT[2]	3_T	**x**	-7,11	y3^{+}-y4^{+}, **y5^{+}, y6^{+}-98, y6^{2+}-98**
photosystem I subunit II, PsaD, Slr0737					
FGGSTGGLLSK	pT[5]	15_T	**x**	30,14	**y3^{+}, y6^{+}, y7^{+}-98,** (y8^{+}, y10^{+})-98
FGGSTGGLLSK	pS[10]	20_S	**x**	31,78	**(y3^{+}, y6^{+}, y7^{+})-98,** (y8^{+}, y10^{+})-98
FGGSTGGLLSK	pS[4]	14_S	**x**	33,04	**y3^{+}, y6^{+}, y7^{+}**, (y8^{+},y10^{+})-98
IGQNPEPVTIKFSGK	pS[13]	134_S		38,01	**y4^{+}-98**, (y7^{+},y9^{+}, y9^{2+})-98, y8^{+}
TELSGQPPK	pT[1]	2_T	**x**	-22,87	**y6^{+}, y7^{+}, y8^{+}, b3^{+}-98**
TELSGQPPK	pS[4]	5_S	**x**	-20,29	**(y6^{+}-y7^{+}), y7^{+}-98, b2^{+}**
photosystem I subunit IV, PsaE, Ssr2831					
SGILYPVIVR	pS[1]	31_S		77,17	**y5^{+}-y6^{+}-y7^{+}, b3^{+}, b3^{+}-98**
photosystem I reaction center subunit III precursor (PSI-F), plastocyanin (cyt c553) docking protein, PsaF, Sll0819					
SKNFLNTTNDPNSGK	pS[1]	42_S		5,54	**y3^{+}, y5^{+}, y8^{+}, y9^{2+}**
photosystem I subunit XI, PsaL, Slr1655					
AESNQVVQAYNGDPFVGH L-STPISDSAFTR	N-Ac-pS[3]	4_S		86,53	y9^{+}, y11^{+}, **y17^{2+}, y24^{2+}, b6^{+}-98**
hypothetical protein, Slr0148					

VAIETNDNLLSGLLGQDLR	pT^{5}	18_T		104,89	$y5^{+}$-$y6^{+}$, **$y9^{+}$-$y10^{+}$**
TLEVITTHNR	pT^{6}	72_T		2,35	**$y4^{+}$**, ($y5^{+}$-$y6^{+}$-$y7^{+}$-$y8^{+}$)-98
water-soluble carotenoid protein, OCP, Slr1963					
IAEPVVPPQDTASR	pT^{11}	182_T	**x**	13,44	**$y3^{+}$**, ($y7^{+}$-$y8^{+}$, $y11^{+}$)-98, $y8^{+}$
IAEPVVPPQDTASR	pS^{13}	184_S	**x**	14,98	($y4^{+}$, $y7^{+}$-$y8^{+}$, $y8^{2+}$)-98, $y8^{+}$
flavodiiron protein, Flv3, Sll0550					
SLDSDLEK	pS^{1}	415_S	**x**	4,95	**$y3^{+}$**-$y4^{+}$**,$y5^{+}$-$y6^{+}$**
SLDSDLEK	pS^{4}	418_S	**x**	13,74	**($y5^{+}$-$y6^{+}$),($y5^{+}$-$y6^{+}$)-98**, **$b3^{+}$**
CAB/ELIP/HLIP-related protein HliD, Ssr1789					
SEELQPNQTPVQEDPK	pS^{1}	2_S		6,97	$y7^{+}$,$y8^{+}$,$y11^{+}$, ($y4^{+}$-$y5^{+}$)-98
ribulose bisphosphate carboxylase large subunit, RbcL, Slr0009					
TFQGPPHGITVER	pT^{1}	142_T		24,07	**$y4^{+}$,$y6^{+}$-$y7^{+}$-$y8^{+}$**, **b3-98**
ribulose bisphosphate carboxylase small subunit, RbcL, Slr0012					
SENPNCYIR	C^{6}, pS^{1}	78_S		8,52	**$y3^{+}$,$y5^{+}$-$y6^{+}$-$y7^{+}$**, **$b3^{+}$-98**

[(a)]Numeration starts from start M in ORF

Phosphopeptide transitions were supplemented with iRT values. The iRT assignment was straightforward for phosphopeptides present as a single isoform, namely for 5 phosphopeptides that contained a single potential modification site, and for 13 ones that contained more than one S/T/Y residue. Other verified phosphopeptides were present in several isoforms. The individual isoforms were differentiated with specific transitions pinpointing the phosphorylation site. In a majority of cases, phosphopeptide isoforms were resolved well during HPLC, like pS^{10} and pS^{6} isomers of ITGNASAIVSNAAR (Figure 4), or only slightly overlapped. Thus, they represent good targets for quantitative studies. The pT^{1} and pS^{7} isoforms of TFDLSPSWYVEALK (CpcA), with 101.66 and 102.64 iRT values, respectively, are the example where peptide peaks overlapped (Figure 5); nevertheless, specific transitions differentiating the two isoforms allowed individual assessment. In contrast, some phosphopeptide isomers had too close iRT values or fully overlapped. The pS^{8}, pS^{9} and pS^{11} isoforms of QPALVGASSDSR from ApcE formed one co-eluting transition group

(Skyline file 1 in the Supporting information). Moreover, while rather intensive non-modified $y2^+$ fragment ion indicated the occurrence of the pS^8 and /or pS^9 isoforms, the presence of the pS^{11} variant was difficult to distinguish due to low intensities of characteristic $y2^+$/$y2^+$-98 and $y3^+$/$y3^+$-98 fragment ions. Similarly, pS^8 and pS^9 was not possible to differentiate in the isoform mixture. The pT^{11} and pS^{13} variants of the IAEPVVPPQDTASR phosphopeptide from OCP are another example of poor resolution (Skyline file 1 in the Supporting information). In addition to close iRT values, 13.44 and 14.98, respectively, the peaks were tailing and most of transitions overlapped in retention time. In these cases, evaluation of individual isoforms was not possible with the SRM approach.

Two phosphorylation sites, pS^1 in SKNFLNTTNDPNSGK (PsaF) and pS^{13} in IGQNPEPVTIKFSGK (PsaD), differ from others. They would not be detected in LC-MS/MS if peptides would be fully digested with trypsin. These phosphopeptides with 1 miscleavage were assessed by SRM to confirm the occurrence of phosphorylation at the specific site. However, they might not be suitable for quantitation purposes since the extent of trypsin miscleavage might be variable between samples.[41]

It is important to underline that SRM validation significantly increased the confidence of identification for phosphorylation sites detected by LC-MS/MS, especially for six of those discovered only once and characterized by a single MS/MS spectrum. Moreover, SRM showed the presence of novel isomeric forms in native samples revealing three additional phosphorylation sites that were missed in LC-MS/MS analysis. Further, SRM helped to clarify problems in resolving of pS^8, pS^9 and pS^{11} isoforms of QPALVGASSDSR from ApcE as well as pT^1 and pS^2 variants of TSLVSAQR from CpcC2. Apparently, the absolute majority of designed transitions supplemented with iRT values shown in Table 1 can be used in future quantitative studies.

From 45 SRM-verified phosphorylation sites in photosynthesis-related proteins, 18 were newly identified in the present study. Some of them belong to four *Synechocystis* 6803 proteins

which, to our knowledge, were not discovered earlier in a phosphorylated form: the PsaF subunit of PSI, the D1 protein of PSII, flavodiiron protein Flv3 and LHC-similar stress-induced protein HliD. Our findings of the three phosphorylation sites at the N-terminus of the D1 protein, Ac-TTTLQQR, shed new light on the controversial issue of the D1 protein phosphorylation in cyanobacteria. In chloroplasts of Arabidopsis thaliana, the phosphorylation at the N-terminus of the D1 protein (Ac-pTAILER) demonstrated by Vener et al.[22] is extensive in high light (about 80% [80]) and plays an important biological role in the turnover of damaged PSII reaction centres by regulating the repair cycle and the migration of impaired PSII complexes from grana stacks to non-appressed stroma-exposed membranes.[81] Cyanobacteria lack grana stacks, and phosphorylated D1 has not been confirmed before.[82] Nevertheless, the phosphorylated residue, T^2, is highly conserved in D1 proteins both in plants and cyanobacteria; in *Synechocystis* 6803, the sequence proceeds with T^3 and T^4. To investigate a possible involvement of the phosphorylation into the D1 turnover in cyanobacteria, Jansson and his colleagues[82,83] have replaced each of the three T with V residues and observed that an introduction of a single mutation has neither affected the water oxidizing machinery of PSII nor the amount or stability of the D1 protein. However, the triple mutant demonstrated reduced growth rate, decreased oxygen evolving activity[82] and perturbation of the energy transfer from PBS to PSII and further to PSI.[83] The results have led to a suggestion that the impairment of PSII in the triple mutant has occurred due to the T->V mutations but not to protein phosphorylation. In contrast, we explicitly demonstrated that all three T in Ac-TTTLQQR can undergo phosphorylation in *Synechocystis* 6803 cells. Our findings helped to explain why the biological effect of mutations generated by Jansson et al.[82] was observed only in the triple mutant where phosphorylation at the D1 N-terminus was not possible. We suggest that the phosphorylation event is needed for a fully functional energy transfer from PBS to PSII but it can occur at any of three T residues. The SRM analysis revealed that the amounts of phosphorylated D1 in our samples were relatively low; however, other environmental conditions like, for example, high light, might

promote more extensive phosphorylation of this protein. Thus, further investigations are required to evaluate biological function of these phosphorylation events, and all three isoforms of the phosphorylated Ac-TTTLQQR peptide should be taken into account.

CONCLUSION

The SRM assays for phosphorylated peptides from *Synechocystis* 6803 proteins involved in light harvesting, photosynthestic electron transfer, photoprotection and carbon fixation will provide novel opportunities to reveal a role of O-phosphorylation in regulation of these important physiological process in cyanobacteria. The SRM assay parameters presented here are deposited to the Panorama Public repository. They are now available for comparisons of the extent of the phosphorylation events in WT and mutant cells challenged with various environmental stresses with an aim to disclose novel regulatory mechanisms for improvement the sustenance and productivity of cyanobacteria cell factories.

ASSOCIATED CONTENT

Supporting information

Supplemental Table : Cover page.

Supplemental Table S1: Calculations of FDR values.

Supplemental Table S2: Phosphopeptides of *Synechocystis* 6803.

Supplemental Table S3: Phosphoproteins of *Synechocystis* 6803 with assigned functions.

Supplemental Table S4: Synthetic “heavy” phosphopeptides analysed by SRM.

Supplemental Table S5: List of transitions used for assessment of the phosphopeptides by SRM.

Supplemental Table S6: CV values of the transitions' areas for phosphopeptides originated from HC- and LC-grown cells.

Supplemental Table S7: Comparison of *Synechocystis* 6803 phosphoproteome data.

Supplemental Figure S1: MS/MS spectra of *Synechocystis* 6803 phosphopeptides detected by LC-MS/MS.

.

Link to the results in the Panorama Public database:

https://panoramaweb.org/labkey/Synechocystis_phospho_photosynthesis_Angeleri_JProtRes_2016.url

Skyline file 1: "Heavy" peptide mixtures.

Skyline file 2: Native unfractionated samples_HC+LC+Mix.

Skyline file 3: Native fractionated samples_Selected peptides.

ACKNOWLEDGEMENTS

The research leading to these results has received funding from the People Programme (Marie Curie Actions) of the European Union's Seventh Framework Programme FP7/2007-2013/under REA Grants Agreement no. 317184. This material reflects only the authors' views and the European Union is not liable for any use that may be made of the information therein. The authors also gratefully acknowledge the financial support from the Academy of Finland Centre of Excellence Project number 271832 (E.M.A.), the Academy of Finland Project number 273870 (E.M.A.), and the Turku University Foundation project number 9925 (N.B.). We thank the Proteomics facility of the Turku Centre for Biotechnology (BTK) for the opportunity to run our MS experiments and for technical support. Authors thank Dr. Susumu Y. Imanishi, Meijo University, Japan, for the valuable discussions.

ABBREVIATIONS

ABC ammonium bicarbonate; AcN Acetonitrile; CV coefficient of variation; Cyt b_6f Cytochrome b_6f; DDA data dependent acquisition; DM n-dodecyl-β-D-maltoside; FA formic acid; FNR ferredoxin:$NADP^+$ oxidoreductase; HCD high energy collision dissociation; HC high carbon; LC low carbon; LC-MS/MS liquid chromatography – tandem mass spectrometry; MS mass spectrometry; NH_3: ammonia; PBS phycobilisomes; PSII photosystem II; PSI photosystem I; PSM peptide spectral match; PTM post translational modification; RT room temperature; Rubisco Ribulose-1,5-bisphosphate carboxylase/oxygenase; SRM selected reaction monitoring; TCEP Tris(2 carboxyethyl)phosphine hydrochloride; TFA trifluoroacetic acid; TSQ triple stage quadrupole.

AUTHOR INFORMATION

Corresponding Author

*Tel: $^+$358 2 3338078 e-mail: natbat@utu.fi.

Notes

The authors declare no competing financial interest.

REFERENCES

1. Abed, R. M.; Dobretsov, S.; Sudesh, K. *J.* Applications of cyanobacteria in biotechnology. *Appl. Microbiol.* **2009**, *106*, 1-12.

2. Grossman, A. R.; Schaefer, M. R.; Chiang, G. G.; Collier, J. L. The phycobilisome, a light harvesting complex responsive to environmental conditions. *Microbiol. Rev.* **1993**, *57*, 725-749.

3. DeRuyter, Y.S.; Fromme, P. Molecular structure of the photosynthetic apparatus. In *Molecular Biology, Genomics and Evolution of Cyanobacteria*; Herrero, A., Flores, E., Eds; Horizon Scientific Press: Norwich, UK, 2008; pp 217–269.

4. Battchikova, N.; Aro, E. Proteomics in revealing the composition, acclimation and biogenesis of thylakoid membranes. In *The Cell Biology of Cyanobacteria*; Herrero, A., Flores, E., Eds; Caister Academic Press: Norfolk, UK, 2014; pp 89-120.

5. Espie, G. S.; Kimber, M. S. Carboxysomes: cyanobacterial RubisCO comes in small packages. *Photosynth. Res.* **2011**, *109*, 7-20.

6. Battchikova, N.; Vainonen, J. P.; Vorontsova, N.; Keränen, M.; Carmel, D.; Aro, E. Dynamic changes in the proteome of *Synechocystis* 6803 in response to CO_2 limitation revealed by quantitative proteomics. *J. Proteome Res.* **2010**, *9*, 5896-5912.

7. Aryal, U. K.; Stöckel, J.; Krovvidi, R. K.; Gritsenko, M. A.; Monroe, M. E.; Moore, R. J.; Koppenaal, D. W.; Smith, R. D.; Pakrasi, H. B.; Jacobs, J. M. Dynamic proteomic profiling of a unicellular cyanobacterium *Cyanothece* ATCC51142 across light dark diurnal cycles. *BMC Syst. Biol.* **2011**, *5*, 194.

8. Vuorijoki, L.; Isojärvi, J.; Kallio, P.; Kouvonen, P.; Aro, E.; Corthals, G.; Jones, P. R.; Muth Pawlak, D. Development of a quantitative SRM based proteomics method to study iron metabolism of *Synechocystis* sp. PCC 6803. *J. Proteome Res.* **2015**, *15*, 266-279.

9. Battchikova, N.; Angeleri, M.; Aro, E. Proteomic approaches in research of cyanobacterial photosynthesis. *Photosynth. Res.* **2015**, *126*, 47-70.

10. Thingholm, T. E.; Jensen, O. N.; Larsen, M. R. Analytical strategies for phosphoproteomics. *Proteomics* **2009**, *9*, 1451-1468.

11. Zhang, C. C.; Gonzalez, L.; Phalip, V. Survey, analysis and genetic organization of genes encoding eukaryotic like signaling proteins on a cyanobacterial genome. *Nucleic Acids Res.* **1998**, *26*, 3619 -3625.

12. Macek, B.; Gnad, F.; Soufi, B.; Kumar, C.; Olsen, J. V.; Mijakovic, I.; Mann, M. Phosphoproteome analysis of *E. coli* reveals evolutionary conservation of bacterial Ser/Thr/Tyr phosphorylation. *Mol. Cell. Proteomics* **2008**, *7*, 299-307.

13. Lévine, A.; Vannier, F.; Absalon, C.; Kuhn, L.; Jackson, P.; Scrivener, E.; Labas, V.; Vinh, J.; Courtney, P.; Garin, J. Analysis of the dynamic *Bacillus subtilis* Ser/Thr/Tyr phosphoproteome implicated in a wide variety of cellular processes. *Proteomics* **2006**, *6*, 2157-2173.

14. Macek, B.; Mijakovic, I.; Olsen, J. V.; Gnad, F.; Kumar, C.; Jensen, P. R.; Mann, The serine/threonine/tyrosine phosphoproteome of the model bacterium *Bacillus subtilis*. M. *Mol. Cell. Proteomics* **2007**, *6*, 697-707.

15. Ravichandran, A.; Sugiyama, N.; Tomita, M.; Swarup, S.; Ishihama, Y. Ser/Thr/Tyr phosphoproteome analysis of pathogenic and non-pathogenic *Pseudomonas* species. *Proteomics* **2009**, *9*, 2764-2775.

16. Parker, J. L.; Jones, A. M.; Serazetdinova, L.; Saalbach, G.; Bibb, M. J.; Naldrett, M. J. Analysis of the phosphoproteome of the multicellular bacterium *Streptomyces coelicolor* A3 (2) by protein/peptide fractionation, phosphopeptide enrichment and high-accuracy mass spectrometry. *Proteomics* **2010**, *10*, 2486-2497.

17. Sanders, C. E.; Melis, A.; Allen, J. F. In vivo phosphorylation of proteins in the cyanobacterium *Synechococcus* 6301 after chromatic acclimation to Photosystem I or Photosystem II light. *Biochim. Biophys. Acta* **1989**, *976*, 168-172.

18. Harrison, M. A.; Tsinoremas, N. F.; Allen, J. F. Cyanobacterial thylakoid membrane proteins are reversibly phosphorylated under plastoquinone-reducing conditions in vitro. *FEBS Lett.* **1991**, 28*2*, 295-299.

19. Mann, N. H.; Newman, J. Phosphorylation of β-phycocyanin in *Synechocystis* sp. PCC 6803. In *The Phototrophic Prokaryotes;* Peschek, G.A.; Löffelhardt, W.; Schmetterer, G.; Eds; Springer: New York, 1999; pp 71-75.

20. Piven, I.; Ajlani, G.; Sokolenko, A. A. Phycobilisome linker proteins are phosphorylated in *Synechocystis* sp. PCC 6803. *J. Biol. Chem.* **2005**, *280,* 21667-21672.

21. Los, D. A.; Zorina, A.; Sinetova, M.; Kryazhov, S.; Mironov, K.; Zinchenko, V. V. Stress sensors and signal transducers in cyanobacteria. *Sensors* **2010**, *10*, 2386-2415.

22. Vener, A. V.; Harms, A.; Sussman, M. R.; Vierstra, R. D. Mass spectrometric resolution of reversible protein phosphorylation in photosynthetic membranes of *Arabidopsis thaliana. J. Biol. Chem.* **2001**, *276,* 6959-6966.

23. Reiland, S.; Messerli, G.; Baerenfaller, K.; Gerrits, B.; Endler, A.; Grossmann, J.; Gruissem, W.; Baginsky, S. Large scale *Arabidopsis* phosphoproteome profiling reveals novel chloroplast kinase substrates and phosphorylation networks. *Plant Physiol.* **2009**, *150,* 889-903.

24. Wang, X.; Bian, Y.; Cheng, K.; Gu, L.; Ye, M.; Zou, H.; Sun, S. S.; He, J. A large scale protein phosphorylation analysis reveals novel phosphorylation motifs and phosphoregulatory networks in *Arabidopsis*. *J. Proteomics* **2013**, 78, 486-498.

25. Tikkanen, M.; Aro, E. Thylakoid protein phosphorylation in dynamic regulation of photosystem II in higher plants. *Biochim. Biophys. Acta* **2012**, *1817,* 232-238.

26. Fristedt, R.; Vener, A. V. High light induced disassembly of photosystem II supercomplexes in *Arabidopsis* requires STN7 dependent phosphorylation of CP29. *PLoS One* **2011**, *6,* e24565.

27. Zorina, A.; Stepanchenko, N.; Novikova, G. V.; Sinetova, M.; Panichkin, V. B.; Moshkov, I. E.; Zinchenko, V. V.; Shestakov, S. V.; Suzuki, I.; Murata, N.; Los, D. A. Eukaryotic like Ser/Thr protein kinases SpkC/F/K are involved in phosphorylation of GroES in the cyanobacterium S*ynechocystis*. *DNA Res.* **2011**, *18,* 137-151.

28. Mikkat, S.; Fulda, S.; Hagemann, M. A 2D gel electrophoresis based snapshot of the phosphoproteome in the cyanobacterium *Synechocystis* sp. strain PCC 6803. *Microbiology* **2014**, *160,* 296-306.

29. Yang, M.; Qiao, Z.; Zhang, W.; Xiong, Q.; Zhang, J.; Li, T.; Ge, F.; Zhao, J. Global phosphoproteomic analysis reveals diverse functions of serine/threonine/tyrosine phosphorylation in the model cyanobacterium *Synechococcus* sp. strain PCC 7002. *J. Proteome Res.* **2013**, *12,* 1909-1923.

30. Spät, P.; Maček, B.; Forchhammer, K. Phosphoproteome of the cyanobacterium *Synechocystis sp*. PCC 6803 and its dynamics during nitrogen starvation. *Front. Microbiol.* **2015**, 6, 248.

31. Chen, Z.; Zhan, J.; Chen, Y.; Yang, M.; He, C.; Ge, F.; Wang, Q. Effects of Phosphorylation of β Subunits of Phycocyanins on State Transition in the Model Cyanobacterium *Synechocystis* sp. PCC 6803. *Plant Cell Physiol.* **2015**, *56,* 1997-2013.

32. Lehmann, W. D.; Krüger, R.; Salek, M.; Hung, C.; Wolschin, F.; Weckwerth, W. Neutral loss based phosphopeptide recognition: a collection of caveats. *J. Proteome Res.* **2007**, *6,* 2866-2873.

33. Cox, J.; Mann, M. MaxQuant enables high peptide identification rates, individualized ppb range mass accuracies and proteome wide protein quantification. *Nat. Biotechnol.* **2008**, *26,* 1367-1372.

34. MacLean, D.; Burrell, M. A.; Studholme, D. J.; Jones, A. M. PhosCalc: a tool for evaluating the sites of peptide phosphorylation from mass spectrometer data. *BMC Research Notes* **2008**, *1,* 30.

35. Martin, D. M.; Nett, I. R.; Vandermoere, F.; Barber, J. D.; Morrice, N. A.; Ferguson, M. A. Prophossi: automating expert validation of phosphopeptide–spectrum matches from tandem mass spectrometry. *Bioinformatics* **2010**, *26,* 2153-2159.

36. Taus, T.; Köcher, T.; Pichler, P.; Paschke, C.; Schmidt, A.; Henrich, C.; Mechtler, K. Universal and confident phosphorylation site localization using phosphoRS. *J. Proteome Res.* **2011**, *10,* 5354-5362.

37. Tyanova, S.; Temu, T.; Carlson, A.; Sinitcyn, P.; Mann, M.; Cox, J. Visualization of LC-MS/MS proteomics data in MaxQuant. *Proteomics* **2015**, *15,* 1453-1456.

38. Riley, N. M.; Coon, J. Phosphoproteomics in the age of rapid and deep proteome profiling. J. *Anal. Chem.* **2015**, *88,* 74-94.

39. Baginsky, S. Protein phosphorylation in chloroplasts–a survey of phosphorylation targets. *J. Exp. Bot.* **2016**, *67,* 3873-3882.

40. Jiang, X.; Han, G.; Feng, S.; Jiang, X.; Ye, M.; Yao, X.; Zou, H. Automatic validation of phosphopeptide identifications by the MS2/MS3 target decoy search strategy. *J. Proteome Res.* **2008**, *7,* 1640-1649.

41. Lange, V.; Picotti, P.; Domon, B.; Aebersold, R. Selected reaction monitoring for quantitative proteomics: a tutorial. *Mol. Syst. Biol.* **2008**, *4*,222..

42. Picotti, P.; Rinner, O.; Stallmach, R.; Dautel, F.; Farrah, T.; Domon, B.; Wenschuh, H.; Aebersold, R. High throughput generation of selected reaction monitoring assays for proteins and proteomes. *Nat. Methods* **2010**, *7,* 43-46.

43. Rost, H. L.; Malmstrom, L.; Aebersold, R. Reproducible quantitative proteotype data matrices for systems biology. *Mol. Biol. Cell* **2015**, *26,* 3926-3931.

44. Afzal, V.; Huang, J. T.; Atrih, A.; Crowther, D. PChopper: high throughput peptide prediction for MRM/SRM transition design. *BMC Bioinformatics* **2011**, 12, 338..

45. Liu, X.; Jin, Z.; O'Brien, R.; Bathon, J.; Dietz, H. C.; Grote, E.; Van Eyk, J. E. Characterization, structure and function of linker polypeptides in phycobilisomes of cyanobacteria and red algae: an overview. *Biochim. Biophys. Acta **2005,** 1708 133-142.*

46. De Graaf, E. L.; Kaplon, J.; Mohammed, S.; Vereijken, L. A.; Duarte, D. P.; Redondo Gallego, L.; Heck, A. J.; Peeper, D. S.; Altelaar, A. M. Signal transduction reaction monitoring deciphers site-specific PI3K-mTOR/MAPK pathway dynamics in oncogene-induced senescence. *J. Proteome Res.* **2015**, *14,* 2906-2914.

47. Williams, J. G. Construction of specific mutations in photosystem II photosynthetic reaction center by genetic engineering methods in *Synechocystis* 6803. *Meth. Enzymol.* **1988**, 167, 766-778.

48. Stanier, R. Y.; Kunisawa, R.; Mandel, M.; Cohen Bazire, G. Purification and properties of unicellular blue green algae (order *Chroococcales*). *Bacteriol. Rev.* **1971**, *35,* 171-205.

49. Wessel, D.; Flügge, U. A method for the quantitative recovery of protein in dilute solution in the presence of detergents and lipids. *Anal. Biochem.* **1984**, *138,* 141-143.

50. Imanishi, S. Y.; Kochin, V.; Eriksson, J. E. Optimization of phosphopeptide elution conditions in immobilized Fe (III) affinity chromatography. *Proteomics* **2007**, *7,* 174-176.

51. Picotti, P.; Aebersold, R. Selected reaction monitoring based proteomics: workflows, potential, pitfalls and future directions. *Nat. Methods* **2012**, *9,* 555-566.

52. MacLean, B.; Tomazela, D. M.; Shulman, N.; Chambers, M.; Finney, G. L.; Frewen, B.; Kern, R.; Tabb, D. L.; Liebler, D. C.; MacCoss, M. J. Skyline: an open source document editor for creating and analyzing targeted proteomics experiments. *Bioinformatics* **2010**, *26,* 966-968.

53. Mann, M.; Ong, S.; Grønborg, M.; Steen, H.; Jensen, O. N.; Pandey, A. Analysis of protein phosphorylation using mass spectrometry: deciphering the phosphoproteome. *Trends Biotechnol.* **2002**, *20,* 261-268.

54. Kersten, B.; Agrawal, G. K.; Iwahashi, H.; Rakwal, R. Plant phosphoproteomics: a long road ahead. *Proteomics* **2006**, *6,* 5517-5528.

55. Wang, F.; Song, C.; Cheng, K.; Jiang, X.; Ye, M.; Zou, H. Perspectives of comprehensive phosphoproteome analysis using shotgun strategy. *Anal. Chem.* **2011**, *83,* 8078-8085.

56. Nakagami, H.; Sugiyama, N.; Ishihama, Y.; Shirasu, K. Shotguns in the front line: phosphoproteomics in plants. *Plant Cell Physiol.* **2012**, *53,* 118-124.

57. Fíla, J.; Honys, D. Enrichment techniques employed in phosphoproteomics. *Amino Acids* **2012**, *43,* 1025-1047.

58. Beltran, L.; Cutillas, P. R. Advances in phosphopeptide enrichment techniques for phosphoproteomics. *Amino Acids* **2012**, 4*3,* 1009-1024.

59. Han, G.; Ye, M.; Zhou, H.; Jiang, X.; Feng, S.; Jiang, X.; Tian, R.; Wan, D.; Zou, H.; Gu, J. Large-scale phosphoproteome analysis of human liver tissue by enrichment and fractionation of phosphopeptides with strong anion exchange chromatography. *Proteomics* **2008**, *8,* 13461361.

60. Nakagami, H.; Sugiyama, N.; Mochida, K.; Daudi, A.; Yoshida, Y.; Toyoda, T.; Tomita, M.; Ishihama, Y.; Shirasu, K. Large scale comparative phosphoproteomics identifies conserved phosphorylation sites in plants. *Plant Physiol.* **2010**, 15*3,* 1161-1174.

61. Silva-Sanchez, C.; Li, H.; Chen, S. Recent advances and challenges in plant phosphoproteomics. *Proteomics* **2015**, *15,* 1127-1141.

62. Cameron, J. C.; Wilson, S. C.; Bernstein, S. L.; Kerfeld, C. A. Biogenesis of a bacterial organelle: the carboxysome assembly pathway. *Cell* **2013**, *155,* 1131-1140.

63. Bantscheff, M.; Schirle, M.; Sweetman, G.; Rick, J.; Kuster, B. Quantitative mass spectrometry in proteomics: a critical review. *Anal. Bioanal. Chem.* **2007**, *389*, 1017-1031.

64. Bantscheff, M.; Lemeer, S.; Savitski, M. M.; Kuster, B. Quantitative mass spectrometry in proteomics: critical review update from 2007 to the present. *Anal. Bioanal. Chem.* **2012**, *404*, 939-965.

65. Ishii, A.; Hihara, Y. An AbrB like transcriptional regulator, Sll0822, is essential for the activation of nitrogen regulated genes in *Synechocystis sp*. PCC 6803. *Plant Physiol.* **2008**, *148*, 660-670.

66. Liu, L.; Chen, X.; Zhang, Y.; Zhou, B. Characterization, structure and function of linker polypeptides in phycobilisomes of cyanobacteria and red algae: an overview. *Biochim. Biophysic. Acta* **2005**, *1708*, 133-142.

67. Chitnis, V. P.; Chitnis, P. R. PsaL subunit is required for the formation of photosystem I trimers in the cyanobacterium *Synechocystis* sp. PCC 6803. *FEBS Lett.* **1993**, *336*, 330-334.

68. Long, B. M.; Tucker, L.; Badger, M. R.; Price, G. D. Functional cyanobacterial beta-carboxysomes have an absolute requirement for both long and short forms of the CcmM protein. *Plant Physiol.* **2010**, *153*, 285-293.

69. Wegener, K. M.; Welsh, E. A.; Thornton, L. E.; Keren, N.; Jacobs, J. M.; Hixson, K. K.; Monroe, M. E.; Camp, D. G.,2nd; Smith, R. D.; Pakrasi, H. B. High sensitivity proteomics assisted discovery of a novel operon involved in the assembly of photosystem II, a membrane protein complex. *J. Biol. Chem.* **2008**, *283*, 27829-27837.

70. Vener, A. V.; Rokka, A.; Fulgosi, H.; Andersson, B.; Herrmann, R. G. A cyclophilin-regulated PP2A-like protein phosphatase in thylakoid membranes of plant chloroplasts. *Biochemistry* **1999**, *38*, 14955-14965.

71. van Wijk, K.J. Plastid proteomics. *Plant Physiol. Biochem.* **2004**, *42*, 963-977.

72. Aro, E. M.; Suorsa, M.; Rokka, A.; Allahverdiyeva, Y.; Paakkarinen, V.; Saleem, A.; Battchikova, N.; Rintamaki, E. Dynamics of photosystem II: a proteomic approach to thylakoid protein complexes. *J. Exp. Bot.* **2005**, *56*, 347-356.

73. Trotta, A.; Suorsa, M.; Rantala, M.; Lundin, B.; Aro, E. Serine and threonine residues of plant STN7 kinase are differentially phosphorylated upon changing light conditions and specifically influence the activity and stability of the kinase. *Plant J.* **2016**, *87*, 484–494 .

74. de Graaf, E. L.; Altelaar, A. M.; van Breukelen, B.; Mohammed, S.; Heck, A. J. Improving SRM assay development: a global comparison between triple quadrupole, ion trap, and higher energy CID peptide fragmentation spectra. *J. Proteome Res.* **2011**, *10*, 4334-4341.

75. Boersema, P. J.; Mohammed, S.; Heck, A. J. Phosphopeptide fragmentation and analysis by mass spectrometry. *J. Mass Spectrom.* **2009**, *44*, 861-878.

76. Wolf Yadlin, A.; Hautaniemi, S.; Lauffenburger, D. A.; White, F. M. Multiple reaction monitoring for robust quantitative proteomic analysis of cellular signaling networks. *Proc. Natl. Acad. Sci. U. S. A.* **2007**, *104*, 5860-5865.

77. Badger, M. R.; Price, G. D.; Long, B. M.; Woodger, F. J. The environmental plasticity and ecological genomics of the cyanobacterial CO_2 concentrating mechanism. *J. Exp. Bot.* **2006**, *57*, 249-265.

78. Burnap, R. L.; Nambudiri, R.; Holland, S. Regulation of the carbon concentrating mechanism in the cyanobacterium *Synechocystis* sp. PCC6803 in response to changing light intensity and inorganic carbon availability. *Photosynth. Res.* **2013**, *118*, 115-124.

79. Burnap, R. L.; Hagemann, M.; Kaplan, A. Regulation of CO_2 concentrating mechanism in cyanobacteria. *Life* **2015**, *5*, 348-371.

80. Rintamaki, E.; Kettunen, R.; Aro, E. M. Differential D1 dephosphorylation in functional and photodamaged photosystem II centers. *J. Biol. Chem.* **1996**, *271*, 14870-14875.

81. Järvi, S.; Suorsa, M.; Aro, E. Photosystem II repair in plant chloroplasts—regulation, assisting proteins and shared components with photosystem II biogenesis. *Biochim. Biophys. Acta* **2015**, *1847*, 900-909.

82. Salih, G.; Jansson, C. Site specific mutations of the N terminal threonines in the D1 protein affects photoautotrophic growth but not D1 protein stability in *Synechocystis* 6803. *Plant Mol. Biol.* **1998**, *36*, 585-591.

83. Funk, C.; Schroëder, W. P.; Salih, G.; Wiklund, R.; Jansson, C. Engineering of N-terminal threonines in the D1 protein impairs photosystem II energy transfer in *Synechocystis* 6803. *FEBS Lett.* **1998**, *436,* 434-438.

Tables

Table 1: List of phosphopeptides and phosphopeptide isoforms distinguished by SRM

Phosphopeptide	Phosphorylation site in peptide	Phosphorylation site in protein[(a)]	Heavy	iRT Value	Ions / **Characteristic ions**
phycocyanin alpha subunit CpcA, Sll1578					
TPLTEAVSTADSQGR	pS[12]	14_S		29,28	**(y4$^+$, y7$^+$ y10$^+$, y12)$^+$ 98**
TPLTEAVSTADSQGR	pS[8]	10_S		37,09	**y4$^+$ y7$^+$, (y8$^+$ y10$^+$) 98**
TPLTEAVSTADSQGR	pT[1]	3_T		41,85	**y4$^+$, y8$^+$, y9$^+$, y12$^+$**
TFDLSPSWYVEALK	pT[1]	121_T		101,66	y6$^+$, **y(9 11)$^+$, b3$^+$ 98**
TFDLSPSWYVEALK	pS[7]	125_S		102,64	y6$^+$, **(y9$^+$ y10$^+$) 98, y9$^+$, b3$^+$**
ANHGLSGDAR	pS[6]	143_S		29,90	y2$^+$, (y6$^+$ y8$^+$) 98
phycocyanin beta subunit CpcB, Sll1577					
ITGNASAIVSNAAR	pS[10]	53_S		16,77	**(y5$^+$ y6$^+$,y8$^+$) 98**, (y9$^+$ y10$^+$) 98
ITGNASAIVSNAAR	pS[6]	49_S		23,79	**y5$^+$ y8$^+$**, (y9$^+$ y10$^+$) 98
GEYLSGSQLDALSATVAEG NKR	pS[7]	22_S		76,84	**y9$^+$ y11$^+$**, (y16^{2+} y18^{2+}) 98, **b5$^+$**
VVSQADAR	pS[3]	10_S		28,08	y4$^+$ y5$^+$, (y6$^+$ y7$^+$) 98
allophycocyanin alpha subunit ApcA,Slr2067					
SLGTPIEAVAQSVR	pS[12]	129_S	**x**	49,17	**(y5$^+$, y7$^+$ y8$^+$, y10$^+$) 98,y10$^+$**
SLGTPIEAVAQSVR	pS[1]	118_S	**x**	82,82	**y7$^+$ y8$^+$, y10$^+$, b3$^+$ 98**
SIVNADAEAR	pS[1]	7_S		9,02	y5$^+$ y8$^+$, b3$^+$ 98
IAETLTGSR	pS[8]	46_S		3,81	**y3 98**, (y5$^+$,y7$^+$ y8$^+$) 98
AFVTGGAAR	pT[4]	31_T		5,58	y5$^+$, (y6$^+$ y7$^+$ y8^{2+}) 98
allophycocyanin beta subunit ApcB, Slr1986					
SYFASGELR	pS[1]	29_S		32,76	**y5$^+$ y7$^+$, b3$^+$ 98**
EVTASLVGADAGK	pS[5]	139_S		17,33	**y6$^+$, y8$^+$, (y9$^+$, y10$^+$) 98**, y11$^+$ 98
phycobilisome rod linker polypeptide LR30, CpcC2, Sll1579					
SFQVYR	pS[1]	168_S		17,15	**y2$^+$ y5$^+$**
TSLVSAQR	pT[1]	2_T	**x**	15,68	**y5$^+$ y7$^+$, b3$^+$ 98**
TSLVSAQR	pS[5]	6_S	**x**	9,44	**y4$^+$, (y5$^+$ y6$^+$) 98**
phycobilisome rod core linker polypeptide LRC, CpcG1, Slr2051					
SINPAANTIPK	pS[1]	224_S		16,92	**y6$^+$,y8$^+$ y9$^+$, y8^{2+}, b3$^+$ 98**
SINPAANTIPK	pT[8]	231_T		23,35	**(y4$^+$ y5$^+$, y7^{2+}) 98, (y6$^+$,y9$^+$)**

phycobilisome core membrane linker polypeptide LCM, ApcE, Slr0335					
FVELGQVSAIR	pS^{8}	698_S		61,72	$(y5^{+}$, $y7^{+}$ $y9^{+})$ 98
QPALVGASSDSR		99_S			
QPALVGASSDSR	pS^{8}:pS^{9}:pS^{11}	100_S	**x**	8,65	$y(y5^{+}$, $y7^{+})$, $(y7^{+}$ $y8^{+})$ 98
QPALVGASSDSR		102_S			
photosystem II D1 protein, PsbA, Slr1311					
TTTLQQRFI	N Ac pT^{3}	4_T	**x**	16,03	$y3^{+}$ $y4^{+}$, **$y5^{+}$ 98**, **$y6^{+}$**
TTTLQQR	N Ac pT^{1}	2_T	**x**	12,36	$y3^{+}$ $y4^{+}$ **$y5^{+}$ $y6^{+}$**
TTTLQQR	N Ac pT^{2}	3_T	**x**	7,11	$y3^{+}$ $y4^{+}$, **$y5^{+}$**, **$y6^{+}$ 98**, **$y6^{2+}$ 98**
photosystem I subunit II, PsaD, Slr0737					
FGGSTGGLLSK	pT^{5}	15_T	**x**	30,14	**$y3^{+}$, $y6^{+}$, $y7^{+}$ 98,** $(y8^{+}$, $y10^{+})$ 98
FGGSTGGLLSK	pS^{10}	20_S	**x**	31,78	**$(y3^{+}$, $y6^{+}$, $y7^{+})$ 98,** $(y8^{+}$, $y10^{+})$ 98
FGGSTGGLLSK	pS^{4}	14_S	**x**	33,04	**$y3^{+}$, $y6^{+}$, $y7^{+}$**, $(y8^{+}$,$y10^{+})$ 98
IGQNPEPVTIKFSGK	pS^{13}	134_S		38,01	**$y4^{+}$ 98**, $(y7^{+}$,$y9^{+}$, $y9^{2+})$ 98, $y8^{+}$
TELSGQPPK	pT^{1}	2_T	**x**	22,87	**$y6^{+}$, $y7^{+}$, $y8^{+}$**, **$b3^{+}$ 98**
TELSGQPPK	pS^{4}	5_S	**x**	20,29	**$(y6^{+}$ $y7^{+})$**, **$y7^{+}$ 98**, **$b2^{+}$**
photosystem I subunit IV, PsaE, Ssr2831					
SGILYPVIVR	pS^{1}	31_S		77,17	**$y5^{+}$ $y6^{+}$ $y7^{+}$**, **$b3^{+}$**, **$b3^{+}$ 98**
photosystem I reaction center subunit III precursor (PSI F), plastocyanin (cyt c553) docking protein, PsaF, Sll0819					
SKNFLNTTNDPNSGK	pS^{1}	42_S		5,54	**$y3^{+}$, $y5^{+}$, $y8^{+}$, $y9^{2+}$**
photosystem I subunit XI, PsaL, Slr1655					
AESNQVVQAYNGDPFVGH L STPISDSAFTR	N Ac pS^{3}	4_S		86,53	$y9^{+}$, $y11^{+}$, **$y17^{2+}$, $y24^{2+}$**, **$b6^{+}$ 98**
hypothetical protein, Slr0148					
VAIETNDNLLSGLLGQDLR	pT^{5}	18_T		104,89	$y5^{+}$ $y6^{+}$, **$y9^{+}$ $y10^{+}$**
TLEVITTHNR	pT^{6}	72_T		2,35	**$y4^{+}$**, $(y5^{+}$ $y6^{+}$ $y7^{+}$ $y8^{+})$ 98
water soluble carotenoid protein, OCP, Slr1963					
IAEPVVPPQDTASR	pT^{11}	182_T	**x**	13,44	**$y3^{+}$**, $(y7^{+}$ $y8^{+}$, $y11^{+})$ 98, $y8^{+}$
IAEPVVPPQDTASR	pS^{13}	184_S	**x**	14,98	$(y4^{+}$, $y7^{+}$ $y8^{+}$, $y8^{2+})$ 98, $y8^{+}$
flavodiiron protein, Flv3, Sll0550					
SLDSDLEK	pS^{1}	415_S	**x**	4,95	**$y3^{+}$** $y4^{+}$**,$y5^{+}$ $y6^{+}$**
SLDSDLEK	pS^{4}	418_S	**x**	13,74	**$(y5^{+}$ $y6^{+})$,$(y5^{+}$ $y6^{+})$ 98**, **$b3^{+}$**
CAB/ELIP/HLIP related protein HliD, Ssr1789					
SEELQPNQTPVQEDPK	pS^{1}	2_S		6,97	$y7^{+}$,$y8^{+}$,$y11^{+}$, $(y4^{+}$ $y5^{+})$ 98

ribulose bisphosphate carboxylase large subunit, RbcL, Slr0009				
TFQGPPHGITVER	pT^{1}	142_T	24,07	**$y4^{+}$,$y6^{+}$ $y7^{+}$ $y8^{+}$, b3 98**
ribulose bisphosphate carboxylase small subunit, RbcL, Slr0012				
SENPNCYIR	C^{6}, pS^{1}	78_S	8,52	**$y3^{+}$,$y5^{+}$ $y6^{+}$ $y7^{+}$, $b3^{+}$ 98**

[(a)]Numeration starts from start M in ORF

Figure legends

Figure 1: Schematic representation of the photosynthetic apparatus in cyanobacteria.

Photosynthesis driven electron flow is shown by red arrows. PQ: plastoquinone. Multi protein complexes involved in light harvesting, photosynthesis and CO_2 fixation are indicated by bold italic. Their subunits and other photosynthesis related proteins that contain phosphopeptides studied in the present paper are shown in red.

Figure 2: Pie chart representations of the functional distribution of phosphoproteins detected by LC MS/MS**.**

Figure 3: Individual spectra for Ac TTTLQQR, the N terminal peptide of the PSII D1 protein.

(A) non phosphorylated peptide, (B-D) three phosphopeptide isoforms.

Figure 4: SRM spectra of pS^7 (A) and pS^4 (B) isoforms of the phosphopeptide ITGNASAIVSNAAR (CpcB).

Isoforms resolved well during HPLC eluting at 22,5 min and 25,1 min, respectively. Common fragment ions for the two forms are shown in black, while the characteristic fragment ions unambiguously localizing modification sites are in red. Retention time values are shown in green.

Figure 5: SRM spectra of two phosphopeptide isoforms of the TFDLSPSWYVEALK (CpcA).

(A) The pT^1 isoform identified by LC MS/MS and confirmed by SRM. (B) The pS^7 isoform revealed by SRM. Common fragment ions for the two forms are shown in black while the characteristic fragment ions are in red. Retention time values are shown in green. (C) Partial overlapping of the two phosphopeptides.

Figures

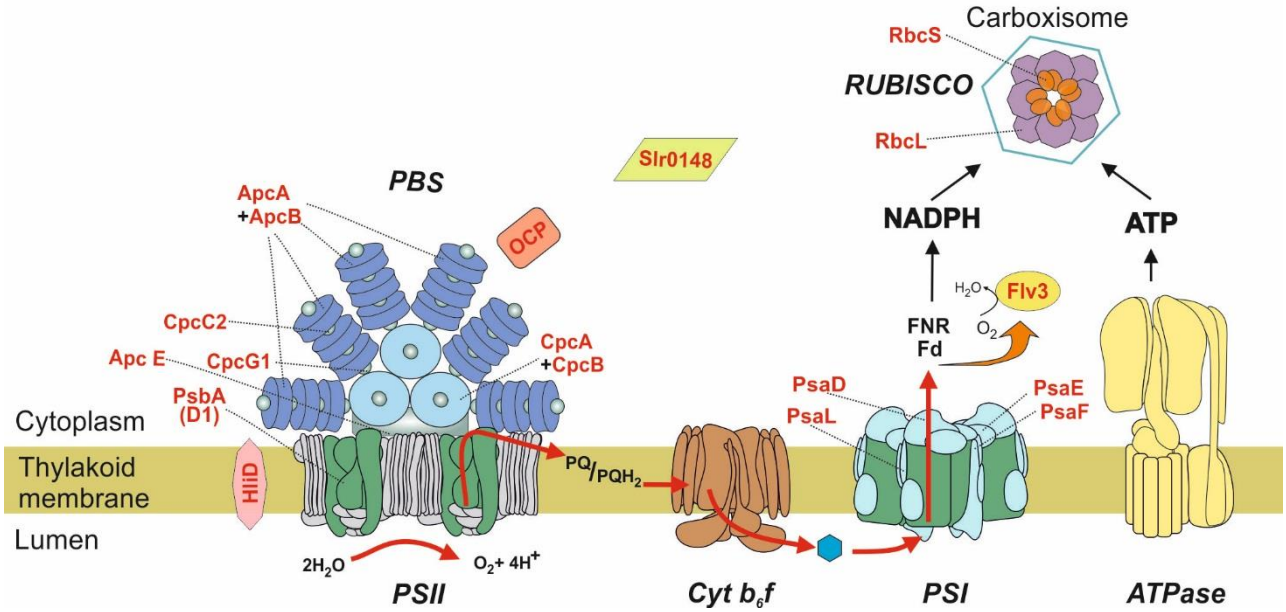

Figure 1

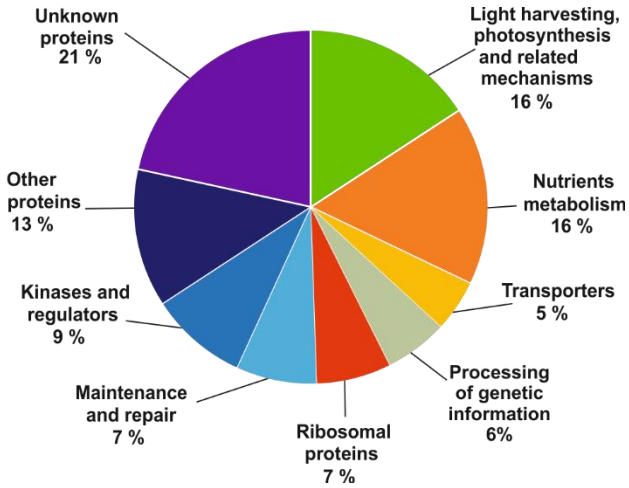

Figure 2

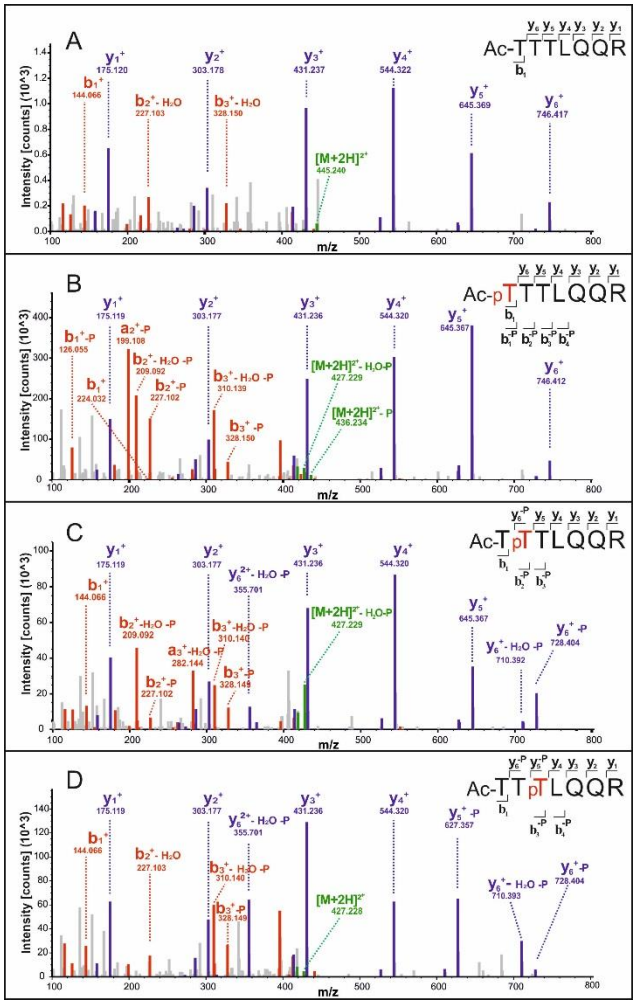
A
Ac-TTTLQQR
B
Ac-pTTTLQQR
C
Ac-TpTTLQQR
D
Ac-TTpTLQQR
Intensity [counts] (10^3)
m/z

Figure 3

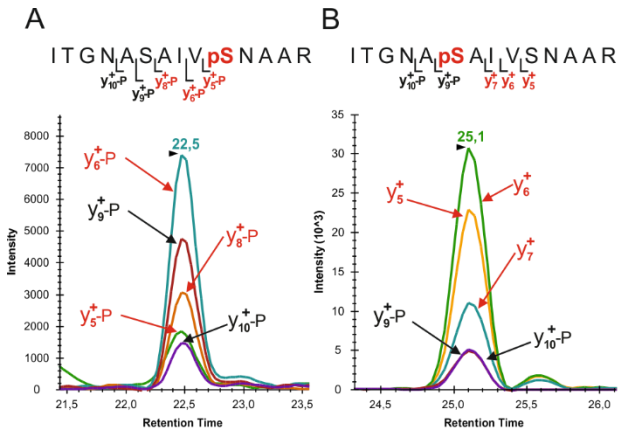

Figure 4

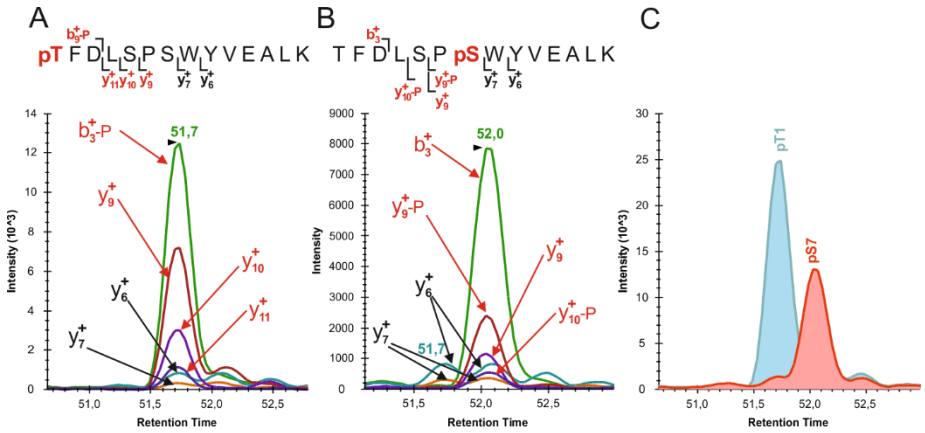

Figure 5

For TOC Only

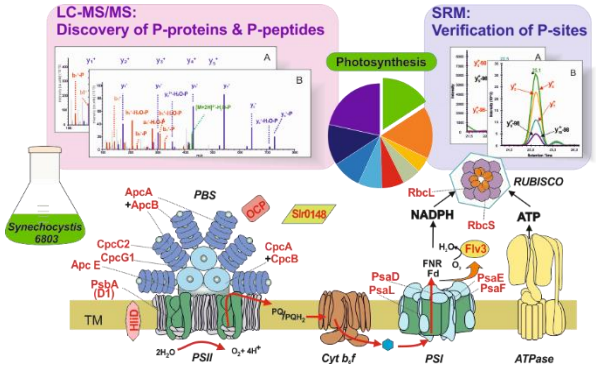
LC-MS/MS:
Discovery of P-proteins & P-peptides
SRM:
Verification of P-sites
Photosynthesis
Synechocystis 6803
PBS
ApcA +ApcB
CpcC2
CpcG1
Apc E
PsbA (D1)
CpcA +CpcB
OCP
Slr0148
TM
HliD
PSII
Cyt b6f
PSI
ATPase
RUBISCO
RbcL
RbcS
NADPH
ATP
Flv3
FNR
Fd
PsaD
PsaL
PsaE
PsaF